RNA interference. K562 cells were cultured in medium containing 1 μM imatinib for 24 h. Cells (2×10^6) were then transfected with 5 μg of double-stranded Cy3-labeled Bim small interfering RNA (siRNA) or control siRNA by using a hemagglutinating virus of Japan (HVJ) envelope (GenomeONE; Ishihara Sangyo Kaisha, Osaka, Japan) according to the manufacturer's directions. Cell culture was continued in the presence of imatinib for 24 h, and then cells were harvested to isolate RNA and cell lysate. Cells were also stained with annexin V-fluorescein isothiocyanate (FITC) (Promega), followed by analysis with flow cytometry. The primers used were the following, according to Reginato et al. (42): control sense, 5′-(GGCUGUAACUUACGUGUACUU)d(TT)-3′; control antisense, 5′-(AAGUACACGUAAGUUACAGCC)d(TT)-3′; Bim sense, 5′-(GACCGAGAAGGUAGACAAUUG)d(TT)-3′; Bim antisense, 5′-(CAAUUGUCUACCUUCUCGGUC)d(TT)-3′.

Immunoblot analysis. Cells were solubilized in Nonidet P-40 lysis buffer (150 mM NaCl, 1.0% Nonidet P-40, 50 mM Tris [pH 8.0]) containing protease inhibitor mixture (Complete; Roche Molecular Biochemicals, Mannheim, Germany); total cellular proteins were separated by sodium dodecyl sulfate-polyacrylamide gel electrophoresis. Cell lysates extracted from 10^5 living cells for hematopoietic progenitors isolated from primary culture or 10^6 living cells for Baf-3 or cell lines established from patients with leukemia were applied to each lane. After their wet electrotransfer onto polyvinylidene difluoride membranes, the proteins were detected with the appropriate antibodies by following standard procedures. The blots were then stained with primary antibodies followed by horseradish peroxidase-conjugated anti-rabbit or anti-mouse immunoglobulin secondary antibodies and subjected to chemiluminescence detection according to the manufacturer's instructions (Amersham, Little Chalfont, Buckinghamshire, United Kingdom). Bim-specific polyclonal antibodies were raised against glutathione *S*-transferase fusion proteins containing amino acids 9 to 53 of mouse BimL, as previously described (44). Bcl-2 and Bcl-x polyclonal antibodies were purchased from Transduction Laboratories (Lexington, Ky.), a monoclonal antibody against β-actin was purchased from Chemicon (Temecula, Calif.), and polyclonal antibodies against total and phosphorylated-specific Akt and MAPK were purchased from Cell Signaling Technology (Beverly, Mass.).

Experiments using Baf-3 cells. Murine IL-3-dependent cells were cultured in RPMI 1640 medium containing 10% fetal calf serum, 20 mM HEPES, 50 μM 2-mercaptoethanol, and 0.5% conditioned medium of 10T1/2 cells as a source of murine IL-3. To deplete IL-3, we washed the cells twice with IL-3-free growth medium. Cell lines established from patients with leukemia were cultured in RPMI 1640 medium supplemented with 10% fetal calf serum. Cell viability was determined by trypan blue dye exclusion. For retrovirus-mediated gene expression, we constructed a control CD8-expressing vector plasmid (pMX/IRES-CD8) from the pMX retroviral vector (a gift of T. Kitamura) (38) by inserting an internal ribosomal entry site (IRES)-CD8 cassette in which the mouse CD8 cDNA was fused in frame to the IRES sequence. The *Bcr-Abl* gene was expressed by inserting the cDNA immediately after the 5′ long terminal repeat sequence. The retrovirus was made by the method described by Onishi et al. (38), using BOSC23 cells. Retroviral infection of Baf-3 cells and the selection of CD8-positive cells with a CD8 monoclonal antibody and MACS separation columns (Miltenyi Biotec) were performed according to a method described previously (27). The selection procedure was repeated until more than 95% of the cells were positive for CD8 by flow cytometry.

Reagents and statistical analysis. A MAPK inhibitor, PD98059 (PD), and a PI3-K inhibitor, LY294002 (LY), were purchased from Wako Pure Chemicals and Sigma-Aldrich (St. Louis, Mo.), respectively. The 2-phenylaminopyrimidine derivative imatinib mesylate was a kind gift of Elisabeth Buchdunger (Novartis, Basel, Switzerland). An analysis of variance and the post hoc method were used to compare viable cell counts in different culture conditions. Significant differences were defined as having a P value of <0.05.

RESULTS

Amplification and isolation of hematopoietic progenitors from mouse bone marrow. We initially tested the role of Bim in the regulation of cell survival by using cytokine-dependent undifferentiated hematopoietic progenitors isolated from primary cultures of bone marrow cells from normal mice. Cells from normal littermates of the Bcr-Abl tg mice (18) were cultured for 5 days in serum-free medium containing 10 ng of TPO per ml and 50 ng of SCF per ml. After the elimination of dead cells, mature granulocytes, and cells expressing lineage-specific markers (CD4, CD8, CD11b, CD41, or Gr-1), more than 90% of the cells were negative for lineage markers and positive for c-Kit (c-Kit$^+$ Lin$^-$). These cells were further divided into Sca-1-enriched fractions (Sca-1$^+$ c-Kit$^+$ Lin$^-$; typically more than 75% of cells were positive for Sca-1 immediately after separation) and Sca-1-depleted fractions (Sca-1$^-$ c-Kit$^+$ Lin$^-$; less than 5% of cells were positive for Sca-1) by using magnetic beads coated with Sca-1 antibody. Figure 1A shows the morphology of Sca-1$^+$ c-Kit$^+$ Lin$^-$ cells. Typical yields of Sca-1-enriched and Sca-1-depleted fractions were 5×10^5 and 2×10^7 cells, respectively, pooled from 10 mice.

Cells in both fractions proliferated and differentiated into mature granulocytes or monocytes when culture was continued in medium containing TPO and SCF (Fig. 1B). Cell numbers increased by around 10-fold by 5 days and then decreased, and cultures died out 10 days later. Although peak cell numbers of the progeny of Sca-1$^+$ c-Kit$^+$ Lin$^-$ cells were always greater than those of Sca-1$^-$ c-Kit$^+$ Lin$^-$ cells, the time courses were similar. When culture was continued in the absence of cytokines, Sca-1$^+$ c-Kit$^+$ Lin$^-$ cells rapidly died within 24 h without maturation (Fig. 1C, left panel). Sca-1$^-$ c-Kit$^+$ Lin$^-$ cells also died but did so more slowly than Sca-1$^+$ c-Kit$^+$ Lin$^-$ cells, and nearly half differentiated into mature granulocytes or monocytes (Fig. 1C, right panel). To confirm that the cell death observed in these experiments was apoptotic, we performed TUNEL assays (Fig. 1D). When Sca-1$^+$ c-Kit$^+$ Lin$^-$ cells were cultured in the presence of cytokines, there was a substantial number in S phase with few TUNEL-positive cells among them (Fig. 1D, left panel). In contrast, in the absence of cytokines, cells underwent G_0/G_1 arrest with many TUNEL-positive cells (Fig. 1D, center and right panels). These results indicated that the cell division and survival of Sca-1-positive early hematopoietic progenitors isolated by this method were cytokine dependent.

Upregulation of Bim and downregulation of Bcl-2 in cytokine-deprived hematopoietic progenitors. To elucidate the contribution of Bcl-2 superfamily members to cytokine-dependent cell survival in hematopoietic progenitors, expression levels of A1, Bad, Bax, Bcl-2, Bcl-x_L, BimEL, Mcl-1, and DP5/Hrk mRNA were assessed by using real-time quantitative RT-PCR technology. In both Sca-1$^+$ c-Kit$^+$ Lin$^-$ and Sca-1$^-$ c-Kit$^+$ Lin$^-$ cells from normal littermates, rapid downregulation of Bcl-2 and upregulation of BimEL were consistently observed in independent experiments (Fig. 2A), while mRNA expression of other Bcl-2 superfamily members did not change significantly upon cytokine deprivation (data not shown). Although downregulation of Bcl-x_L following cytokine deprivation has been observed in many cytokine-dependent cell lines, including Baf-3, FL5.12, and 32D (27, 28, 39), Bcl-x_L expression in hematopoietic progenitors isolated by this method was not affected by cytokine deprivation (Fig. 2A). These findings were further supported at the protein level by immunoblot analysis (Fig. 2B); simultaneous downregulation of Bcl-2 and upregulation of BimEL were observed, while Bcl-x_L remained unchanged in both Sca-1$^+$ c-Kit$^+$ Lin$^-$ and Sca-1$^-$ c-Kit$^+$ Lin$^-$ cells. Importantly, the levels of the two antiapoptotic Bcl-2 family members Bcl-x_L and Bcl-2 were 5- to 10-fold lower in Sca-1$^+$ c-Kit$^+$ Lin$^-$ cells than in Sca-1$^-$ c-Kit$^+$ Lin$^-$ cells, possibly explaining the rapid apoptosis observed in the former (Fig. 1C). These results suggest that the induction

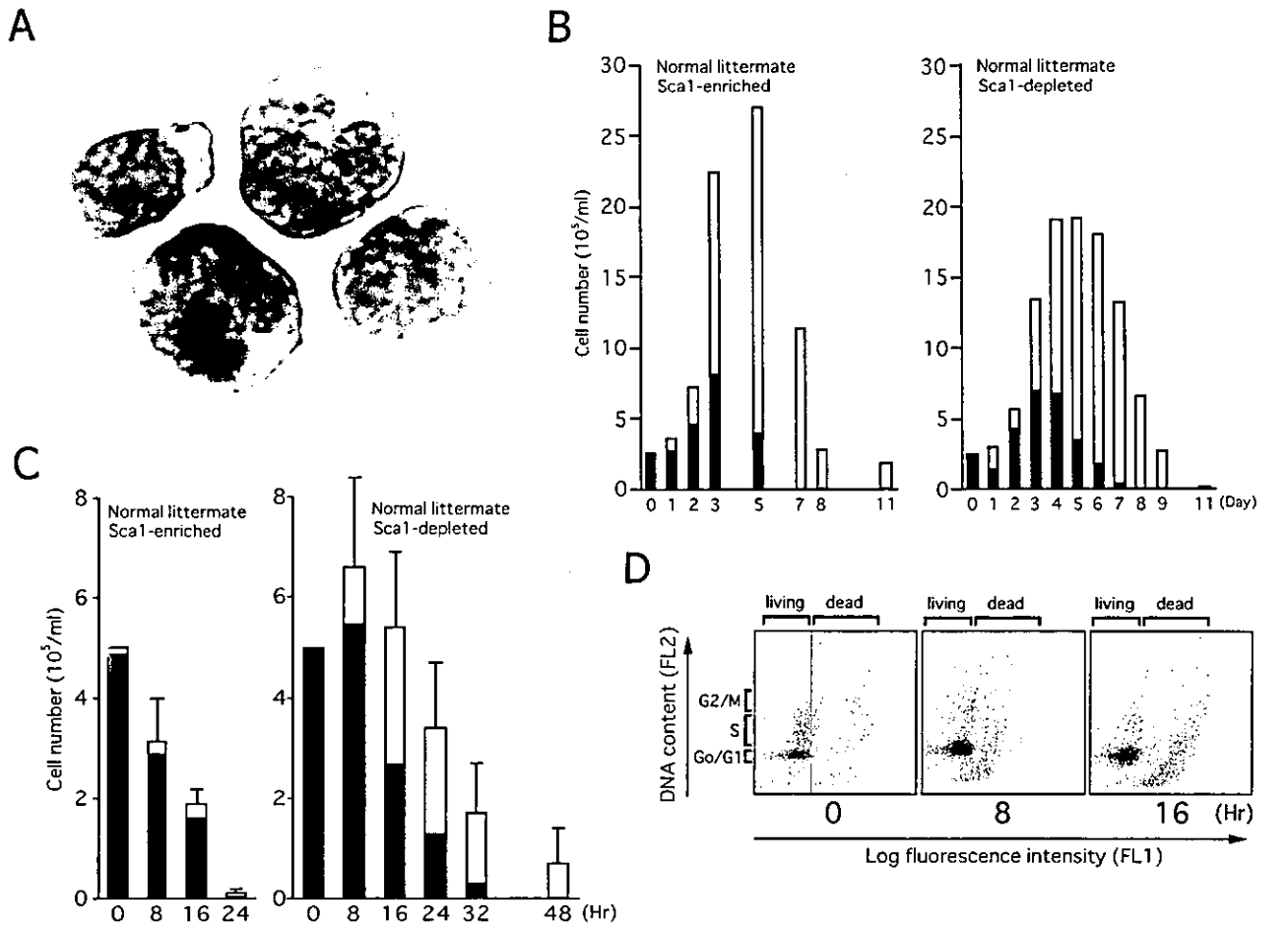

FIG. 1. Cytokine-dependent hematopoietic progenitors isolated from mouse bone marrow. (A) Cytospin preparation showing the morphology of Sca-1-positive early hematopoietic progenitors (Sca-1$^+$ c-Kit$^+$ Lin$^-$) isolated from primary cultures of mouse bone marrow cells visualized by May-Giemsa staining. (B and C) Cultures of Sca-1$^+$ c-Kit$^+$ Lin$^-$ (left panels) and Sca-1$^-$ c-Kit$^+$ Lin$^-$ cells (right panels) were continued in the presence (B) or absence (C) of SCF and TPO. The numbers of viable cells were determined by trypan blue dye exclusion. Blast cells (black bars) and terminally differentiated cells (open bars) were quantified by cytospin centrifugation. Results from one representative study (B) and the means and standard errors of results from three independent experiments (C) are shown. (D) Sca-1$^+$ c-Kit$^+$ Lin$^-$ cells were cultured in cytokine-free medium for the indicated periods. Cells were harvested, the TUNEL assay was performed with fluorescein-dUTP, and cells were stained with propidium iodide. Cytospin preparations were made and analyzed with a laser cytoscan.

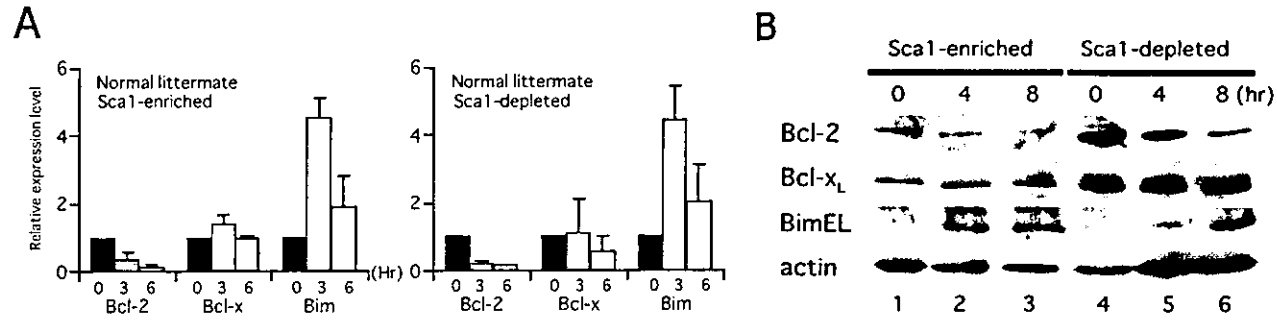

FIG. 2. Expression of Bcl-2, Bcl-x_L, and BimEL in Sca-1$^+$ c-Kit$^+$ Lin$^-$ and Sca-1$^-$ c-Kit$^+$ Lin$^-$ cells from normal mice. Cells were cultured in the absence of cytokines for the indicated times. (A) Real-time quantitative PCR was carried out, and the numbers of cycles required to produce a detectable product were measured and used to calculate differences (n-fold) in starting mRNA levels for each sample by using 28S rRNA as an internal control. mRNA expression levels in cells cultured for 0 (black bars), 3 (gray bars), and 6 (open bars) h without cytokines relative to those in cells cultured in the presence of cytokines are shown. (B) Protein expression levels of the three Bcl-2 superfamily members, as well as β-actin as a control for equal loading, were analyzed by immunoblotting with specific antibodies for each protein.

of Bim by cytokine deprivation plays an important role in regulating cell fate in Sca-1-positive early progenitors.

Bcr-Abl reverses the upregulation of Bim by IL-3 deprivation in IL-3-dependent cells. To test whether Bcr-Abl downregulates Bim expression, we initially used Baf-3 cells expressing Bcr-Abl. Baf-3 cells were infected with retrovirus containing Bcr-Abl and mouse CD8 cDNA as a marker (pMX-Bcr-Abl/IRES-CD8; see Materials and Methods), and infected cells were selected with magnetic beads coated with CD8 antibodies. As reported by others (11, 28), these cells proliferated in IL-3-free medium at nearly the same rate as they did in IL-3-containing medium (data not shown). As previously reported (13, 44), the simultaneous downregulation of Bcl-x_L and upregulation of Bim were induced by IL-3 starvation in wild-type Baf-3 cells (Fig. 3A). In Baf-3 cells expressing Bcr-Abl, Bcl-x_L expression levels were unaffected, while Bim protein was induced for 12 h after IL-3 deprivation, and then the level of Bim declined and returned to its original level within 3 days (Fig. 3B). It was also reported previously that BimEL is phosphorylated by IL-3 signaling (44), shown here by slower migrating bands (Fig. 3A, lane 1, and C, top blot). Similar slower migrating bands were observed in Baf-3 cells expressing Bcr-Abl in the absence of IL-3 [Fig. 3B and C, blots labeled Bim and Baf-3 (Bcr-Abl)], suggesting that Bcr-Abl also phosphorylates BimEL.

In wild-type Baf-3 cells, it was demonstrated previously that signals from the distal portion of the βc chain independently downregulate Bim expression through both the classical Ras/Raf/MAPK and Ras/PI3-K pathways (44). To test whether Bcr-Abl downregulates Bim expression via the same signaling pathways in this particular cell system, Baf-3 cells expressing Bcr-Abl were cultured in the absence of IL-3 for 3 days, after which they were treated with the MAPK inhibitor PD, the PI3-K inhibitor LY, or both. The effects of these inhibitors were monitored by immunoblot analysis using antibodies recognizing phosphorylated Akt (pAkt) or phosphorylated MAPK. When cells were treated with PD, phosphorylated MAPK but not pAkt decreased, and viability was slightly reduced (Fig. 3D and E). When cells were treated with LY or both PD and LY together, levels of pAkt decreased, and massive cell death occurred. Immunoblot analysis revealed a mild enhancement of Bim expression in cells treated with PD, while a marked elevation was observed in cells treated with LY or both kinase inhibitors (Fig. 3F). These results suggest that, although both Raf/MAPK and PI3-K pathways contribute to cell survival and the downregulation of Bim by Bcr-Abl kinase, PI3-K pathways are more important than Raf/MAPK pathways in this particular cell system.

Bim expression is downregulated in cells expressing Bcr-Abl from patients with leukemia. To gain insight into the roles of Bim in the process of human leukemogenesis, we quantified the levels of Bim and Bcl-x_L proteins in cell lines established from patients in the BC phase of CML (CML/BC) and from patients with Philadelphia chromosome (Ph^1)-positive acute lymphoblastic leukemia (ALL) and compared them with the levels in patients with human acute myeloid leukemia (AML) and ALL cell lines that do not express the *Bcr-Abl* fusion gene. Levels of Bim in all six cell lines established from patients in CML/BC were low (Fig. 4A, lanes 1 to 6) compared with those in three control AML cell lines (Fig. 4A, lanes 7 to 9). Low levels of Bim, especially BimEL, in Ph^1-positive cells were also observed in five cell lines established from patients with ALL (Fig. 4B, lanes 1 to 5). In contrast, levels of Bcl-x_L varied among cell lines established from patients in CML/BC and patients with AML (Fig. 4A), as expected based on results from previous studies reporting that Bcl-x_L expression levels differ among AML patients (43). The levels of Bcl-x_L in all ALL cell lines with or without Bcr-Abl expression seemed consistently low compared with those in AML cell lines (Fig. 4B).

To test whether the low level of Bim protein expression in Ph^1-positive leukemia cells was due to the potential of Bcr-Abl tyrosine kinase to downregulate it (as shown in Fig. 3B), we blocked Bcr-Abl function by using a specific inhibitor of Abl kinase, imatinib mesylate (formerly known as STI571). As previously reported (12, 24), apoptosis was induced by imatinib in five cell lines established from patients in CML/BC, and dephosphorylation of Akt and MAPK was observed in these cells (Fig. 5A and B). Increased levels of Bim proteins, especially BimEL and BimL, were induced by the addition of imatinib to KOPM30, K562, and BV173 cells (Fig. 5C). Moreover, dephosphorylation of BimEL was observed (Fig. 3C), suggesting that Bcr-Abl phosphorylates BimEL or BimL in human Ph^1-positive leukemia cells. Expression levels of Bcl-x_L were not altered in KOPM30 and were downregulated only transiently in K562 and BV173 cells (Fig. 5C). Similar results were obtained with KOPM28 and KOPM53 (data not shown).

To examine whether the upregulation of Bim expression contributes to apoptosis induced by imatinib, K562 cells were transfected with Cy3-labeled siRNA oligonucleotides homologous to the *Bim* sequence or control siRNA (42). The induction efficiency was judged to be around 60% based on observations with fluorescence microscopy (data not shown). Real-time quantitative RT-PCR analysis using a primer set to cross the cleavage site [Bim(si)] (Table 1) revealed a 45% reduction of Bim mRNA by the Bim siRNA when whole cells were analyzed (Fig. 5D, left panel). Immunoblot analysis revealed a greater-than-60% reduction of Bim protein, while Bcl-x_L analyzed as a control was reduced by less than 10% (Fig. 5D, right panel). The percentage of apoptotic cells was determined with annexin V-FITC. Cells transfected with Bim siRNA showed a significantly lower percentage of annexin V-positive cells (68.1% ± 7.3% [average ± standard deviation]) than those transfected with control siRNA (38.1% ± 9.3%) (Fig. 5E). These data suggest that Bcr-Abl supports cell survival in cell lines established from patients in CML/BC through the downregulation of Bim, although it was not clear whether the magnitude of Bim induction in these cells was sufficient to account for all of the apoptosis caused by imatinib.

Prolonged survival of Sca-1-positive early progenitors from Bcr-Abl tg mice in cytokine-free medium. Cell lines established with cells in CML/BC harbor additional abnormalities that develop during progression to BC and/or during adaptation to the ex vivo artificial culture environment. To test whether Bcr-Abl downregulates Bim expression in cells from patients in the chronic phase of CML, we used progenitors expressing Bcr-Abl from primary cultures of bone marrow cells obtained from Bcr-Abl tg mice that always develop CML-like myeloproliferative disease (see the introduction). Their survival and

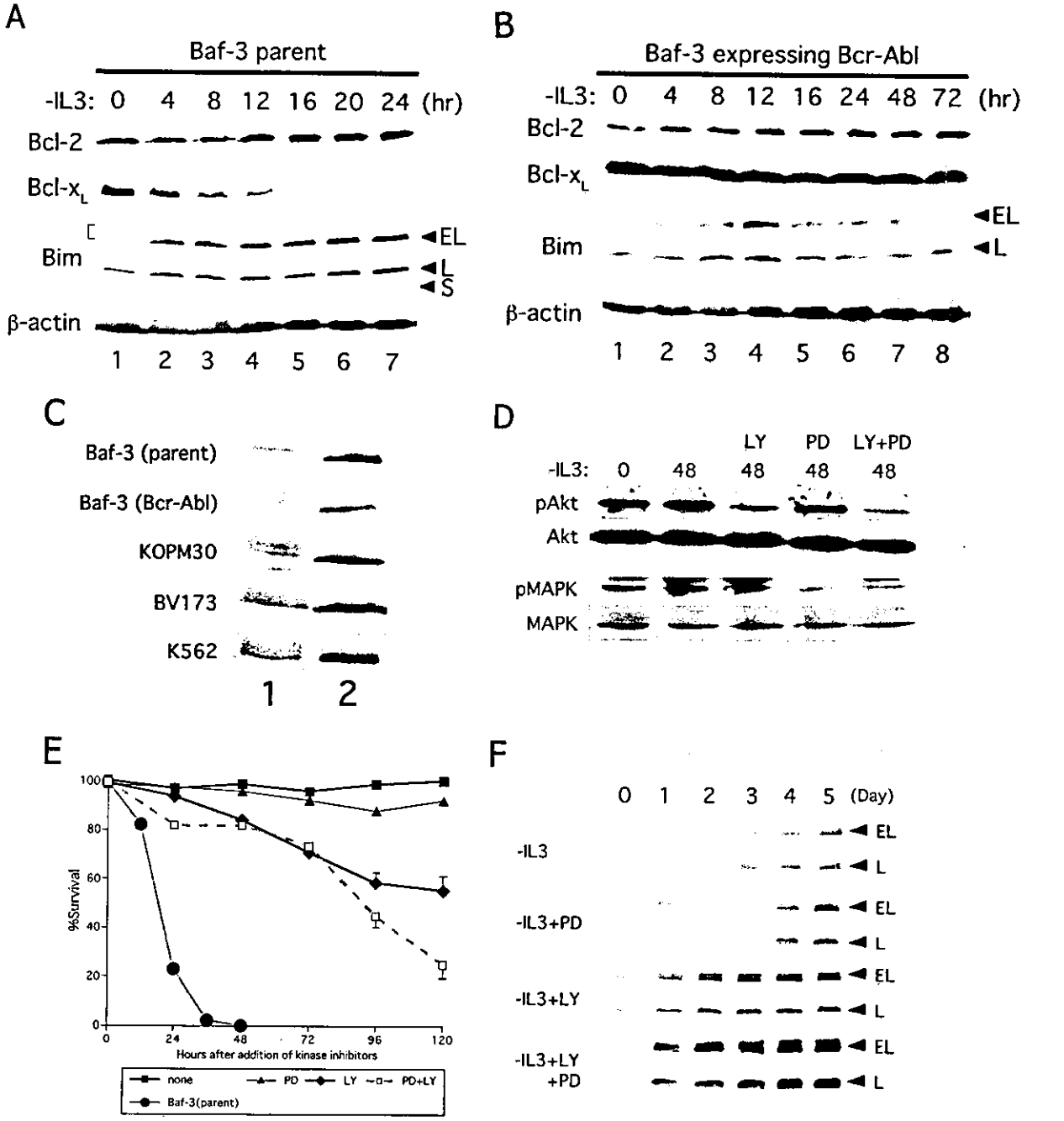

FIG. 3. Bim expression is regulated by IL-3 or Bcr-Abl through Raf/MAPK and/or PI3-K pathways in Baf-3 cells. EL, BimEL; L, BimL; S, BimS. (A and B) Expression of Bcl-2, Bcl-x_L, and Bim proteins in wild-type Baf-3 cells (A) and Baf-3 cells expressing Bcr-Abl after infection with a retrovirus vector (B). Cells were cultured in the absence of IL-3 for the indicated times. An immunoblot analysis using antibody specific for each protein was performed. A bracket in panel A indicates the phosphorylated forms of BimEL. (C) Phosphorylation of BimEL protein. Parental Baf-3 cells were cultured in the presence of IL-3 (lane 1) or in the absence of IL-3 (lane 2) for 4 h; IL-3-starved and Bcr-Abl expressing Baf-3, KOPM30, BV173, and K562 cells were cultured in the absence (lane 1) or presence (lane 2) of imatinib for 12 h. (D to F) Baf-3 cells expressing Bcr-Abl were cultured in IL-3-free medium for 72 h and then treated with PD, LY, or both (LY+PD) at a concentration of 50 μM for the indicated times (in hours). Immunoblot analyses using anti-phosphorylated form-specific Akt or MAPK, as well as antibodies recognizing total Akt or MAPK (D) or anti-Bim antibody (F), were performed. (E) Cell viability was determined by trypan blue dye exclusion. The survival curve of parental Baf-3 cells is shown as a control. Standard errors are shown when they were greater than 3%.

levels of Bcl-2 superfamily member expression were compared with those of their normal littermates.

Sca-1$^+$ c-Kit$^+$ Lin$^-$ and Sca-1$^-$ c-Kit$^+$ Lin$^-$ cells were isolated from primary cultures of bone marrow cells from the tg mice. When these cells were cultured in the presence of cytokines, they proliferated with kinetics similar to those of cells from the normal littermates of the tg mice (Fig. 6A), although cell numbers from the tg mice were greater than those from

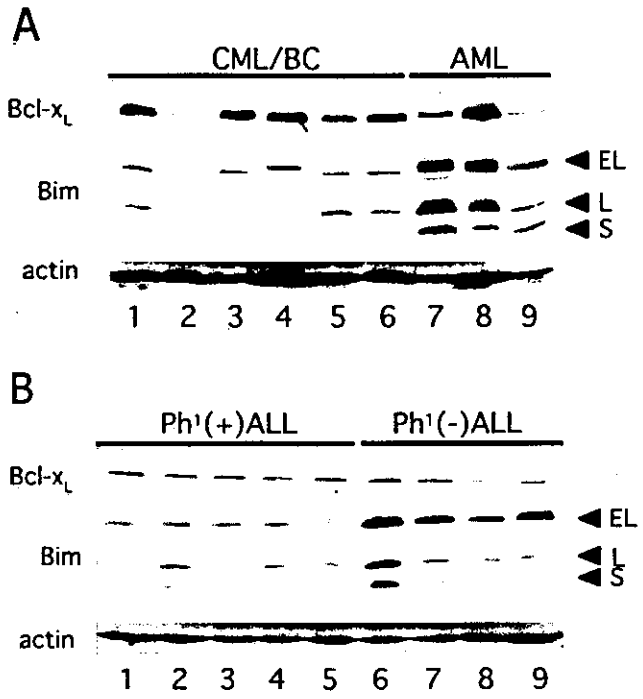

FIG. 4. Levels of Bcl-x_L and Bim protein in human leukemia cell lines. Immunoblot analysis using antibody specific for each protein was performed. EL, BimEL; L, BimL; S, BimS. (A) Lanes 1 to 6, the KOPM28, KOPM30, KOPM53, K562, BV173, and KU812 cell lines, respectively, established with CML/BC cells; lanes 7 to 9, the HL60 myeloid leukemia, HEL erythroid leukemia, and U937 monocytic leukemia cell lines, respectively, lacking Ph^1. (B) Lanes 1 to 5, the KOPN-55bi, KOPN-57bi, KOPN-66bi, KOPN-72bi, and KOPN-30bi Ph^1-positive pro-B ALL cell lines, respectively; lanes 6 to 9, the 920, 697, RS4;11, and UOC-B1 pro-B ALL cell lines, respectively, lacking Ph^1.

their normal littermates in both fractions (Fig. 1B). When Sca-1$^+$ c-Kit$^+$ Lin$^-$ cells were cultured in cytokine-free medium, they survived for more than 3 days (Fig. 6B, left panel), much longer than those from normal littermates (Fig. 1C, left panel). Indeed, virtually no viable cells from normal littermates were observed 24 h after cytokine deprivation, while cells with immature and mature morphology from Bcr-Abl tg mice survived even after 48 h in repeated experiments. In contrast, Sca-1$^-$ c-Kit$^+$ Lin$^-$ cells underwent apoptosis with kinetics similar to those of cells from the normal littermates (Fig. 1C, right panel). To confirm that Bcr-Abl prolongs the survival of Sca-1-positive early hematopoietic progenitors in cytokine-free medium, we added 1 μM imatinib to the culture medium. Imatinib did not affect the survival of the Sca-1$^-$ c-Kit$^+$ Lin$^-$ cells (Fig. 6C, middle panel). In contrast, Sca-1$^+$ c-Kit$^+$ Lin$^-$ cells rapidly underwent apoptosis (Fig. 6C, left panel). A comparison of the numbers of living cells with those of Sca-1$^+$ c-Kit$^+$ Lin$^-$ cells from normal mice (Fig. 1C) revealed that imatinib seemed not only to reverse the antiapoptotic effects of Bcr-Abl but even to enhance apoptosis at 8 and 16 h. This finding might be explained in part by the inhibitory effects of imatinib against c-Kit function, which could persist after the removal of SCF because imatinib also induced apoptosis in Sca-1$^+$ c-Kit$^+$ Lin$^-$ cells from normal mice at 8 h (not statistically significant; $P = 0.14$) and 16 h ($P < 0.05$) after the removal of the cytokines (Fig. 6C, right panel). These data suggest that Bcr-Abl protects Sca-1-positive early progenitors, but not Sca-1$^-$ c-Kit$^+$ Lin$^-$ cells, from apoptosis caused by cytokine deprivation. Bcr-Abl mRNA expression was detected by RT-PCR in both fractions (data not shown).

Suppression of Bim induction in cytokine-deprived progenitors by Bcr-Abl. To clarify the mechanism through which Bcr-Abl prolongs survival of Sca-1-positive progenitors, we assessed the expression of Bcl-2 superfamily members in these cells. Real-time quantitative RT-PCR revealed that neither Bcl-2, Bcl-x_L, nor Bim mRNA expression was altered by cytokine deprivation in either Sca-1-positive or Sca-1-negative cells, except that Bim mRNA was induced twofold in Sca-1$^-$ c-Kit$^+$ Lin$^-$ cells (Fig. 7A). These data were confirmed at the protein level by immunoblot analysis. Bcl-2 and Bcl-x_L levels were unchanged by cytokine deprivation, while Bim protein was barely detectable in either fraction (Fig. 7B), in contrast to a clear induction of Bim and downregulation of Bcl-2 in progenitors from normal littermates (Fig. 2B).

To further confirm that Bcr-Abl downregulates Bim, we analyzed the expression of the Bcl-2 superfamily members in cells cultured in cytokine-free medium in the presence of imatinib. Bim was markedly induced, while Bcl-2 was downregulated in Sca-1-positive and -negative progenitors isolated from Bcr-Abl tg mice (Fig. 7C, left and center panels). In contrast, induction levels of Bim in Sca-1-positive progenitors isolated from normal littermates were not changed by treatment with imatinib (Fig. 7C, right panel, and 2A, left panel), suggesting that the reduction of viable cells in progenitors from normal littermates by imatinib (Fig. 6C, right panel) was due to mechanisms other than Bim induction. Taken together, these data indicate that Bcr-Abl reverses the downregulation of Bcl-2 and upregulation of Bim that are observed in cytokine-starved normal hematopoietic progenitors.

DISCUSSION

In earlier studies, it was established that the induction of Bim is an important step in Baf-3 cells undergoing apoptosis due to IL-3 deprivation (44). Here we demonstrate that Bim was induced by cytokine starvation in early hematopoietic progenitors (Sca-1$^+$ c-Kit$^+$ Lin$^-$) isolated by primary short-term culture of bone marrow cells from normal mice. In contrast, Bim was not induced by cytokine starvation in early progenitors from CML model mice that were more resistant to apoptosis than those from normal mice. We also found that Bcr-Abl downregulates Bim expression in Baf-3 cells and cell lines established with cells from patients with Ph^1-positive leukemia, suggesting that Bim is one of the key target factors downstream of Bcr-Abl that render CML progenitors resistant to apoptosis caused by cytokine deprivation.

The function of Bim is reported to be regulated by at least four different mechanisms. First, mRNA expression is downregulated by cytokines in mouse IL-3-dependent Baf-3, FL5.12, and 32D cells through the Ras/MAPK and PI3-K pathways, independently (13, 44). Moreover, NGF suppresses Bim mRNA expression through the inactivation of the c-jun NH_2-terminal kinase in NGF-dependent neuronal cells, including primary cultures of rat sympathetic neurons and neuronally differentiated PC-12 cells (5, 40, 49). In addition, serum depri-

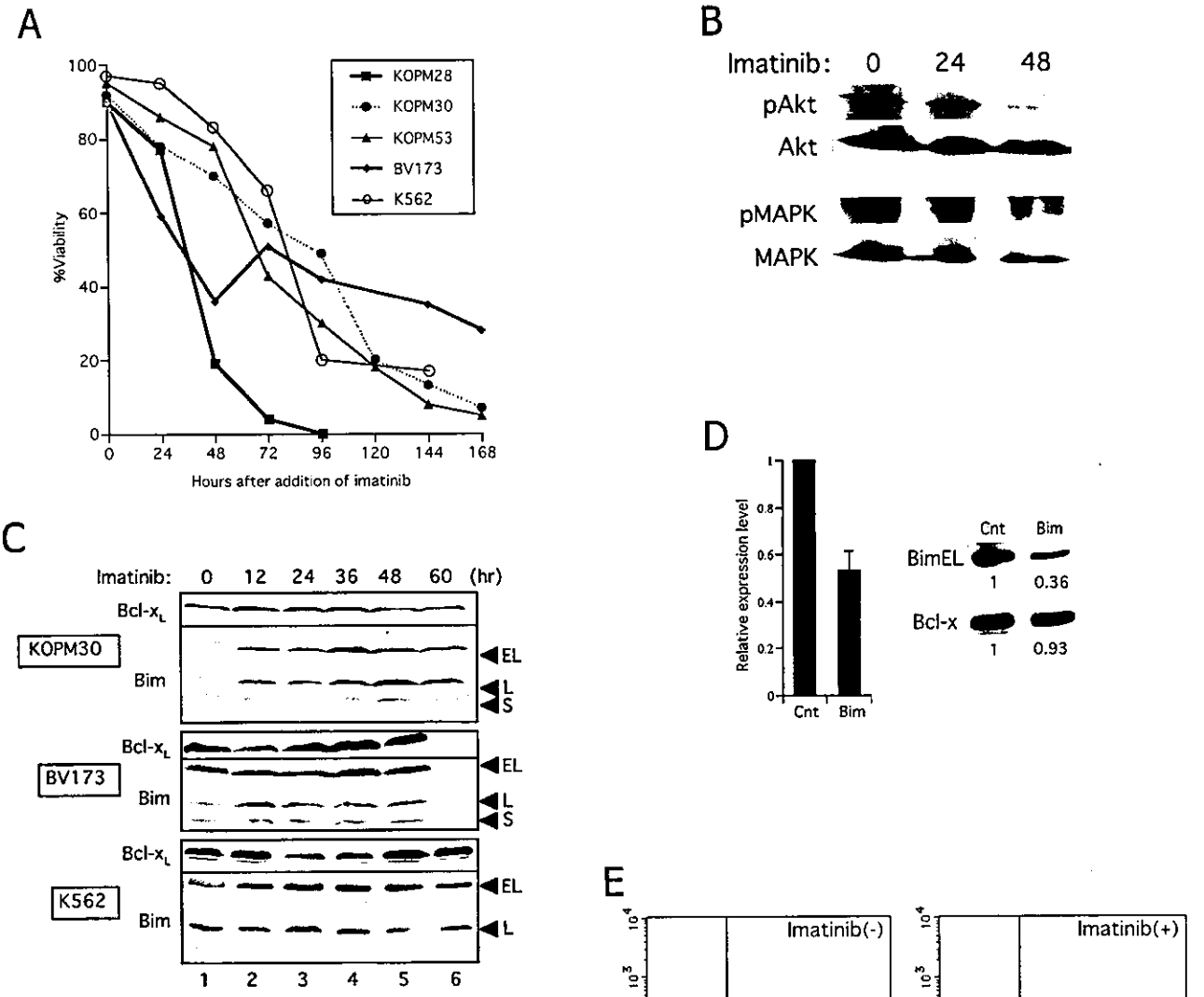

FIG. 5. Effects of imatinib on cell lines established with CML/BC cells. (A) Cell lines (KOPM28, KOPM30, KOPM53, BV173, and K562) established with cells from CML/BC patients were cultured in medium containing imatinib at a concentration of 1 μM for the indicated times. Viability was determined by trypan blue dye exclusion. (B) Immunoblot analyses of K562 cell lysate using anti-phosphorylated form-specific Akt or MAPK, as well as antibodies recognizing total Akt or MAPK, were performed. (C) Levels of Bcl-x_L and Bim proteins in KOPM30, BV173, and K562 cells were determined by immunoblot analysis. EL, BimEL; L, BimL; S, BimS. (D) K562 cells transfected with either Bim siRNA (Bim) or control siRNA (Cnt) were cultured in the presence of 1 μM imatinib for 48 h. The results of real-time RT-PCR using the Bim(si) primers (left panel) and an immunoblot analysis using antibodies specific for Bim (upper right panel) or Bcl-x_L (lower right panel) are shown. Numbers below the immunoblots indicate the relative intensity of each band measured by densitometry. (E) K562 cells were cultured in the absence of imatinib (upper left panel), the presence of 1 μM imatinib for 48 h with mock transfection (upper right panel), Cy3-labeled control siRNA (lower left panel), or Cy3-labeled Bim siRNA (lower right panel). Cells were stained with annexin V-FITC and analyzed by flow cytometry.

vation of CC139 fibroblasts upregulates Bim mRNA via the classical MEK/extracellular signal-regulated kinase (ERK) pathway (48). Second, subcellular localization of Bim is controlled by IL-3 in FDC-P1 cells, another mouse IL-3-dependent line, and by exposure to UV light in 293 cells (29, 41). BimEL and BimL, but not BimS, form complexes with an 8,000-molecular-weight dynein light chain, LC8 (also PIN or Dlc-1) (10, 21, 25). The Bim/LC8 complex in the presence of

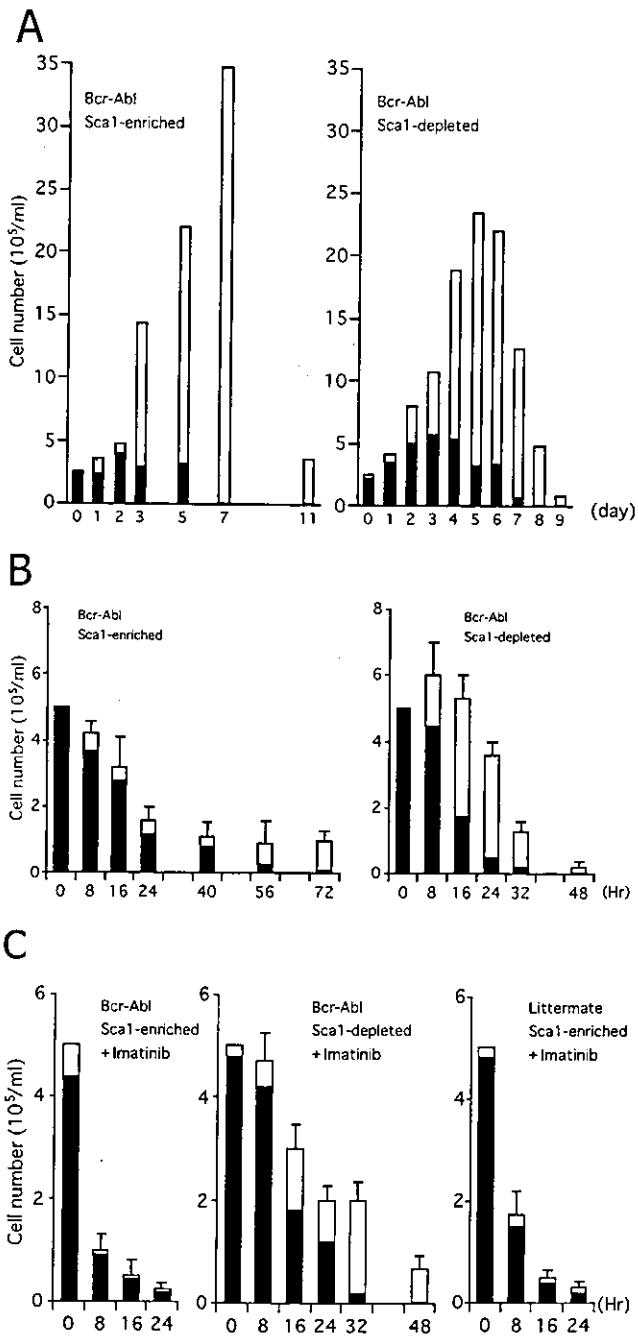

FIG. 6. (A and B) Sca-1$^+$ c-Kit$^+$ Lin$^-$ cells (left panel) and Sca-1$^-$ c-Kit$^+$ Lin$^-$ cells (right panel) amplified and isolated by primary cultures of bone marrow cells from Bcr-Abl tg mice were cultured in the presence (A) or absence (B) of SCF and TPO. (C) Sca-1$^+$ c-Kit$^+$ Lin$^-$ cells (left and right panels) or Sca-1$^-$ c-Kit$^+$ Lin$^-$ cells (middle panel) amplified and isolated by primary cultures of bone marrow cells from Bcr-Abl tg mice (left and middle panels) or their normal littermates (right panel) were cultured in the absence of SCF and TPO. Imatinib was added at a concentration of 1 μM. The number of viable cells was determined by trypan blue dye exclusion. Blast cells (black bars) and terminally differentiated cells (open bars) were determined by cytospin centrifugation. The results from one representative study (A) or the means + standard errors of results from three independent experiments (B and C) are shown.

IL-3 binds to the intermediate chain of the dynein motor complex on the microtubules. IL-3 withdrawal releases the complex from sequestration in the cytoplasm by mechanisms not yet fully understood. In the case of 293 cells exposed to UV, phosphorylation at Thr-56 of (human) BimL by activated c-jun NH_2-terminal kinase was reported to play an important role in this process (29). Third, NGF phosphorylates BimEL and BimL but not BimS through the MEK/MAPK pathway in neuronally differentiated PC-12 cells. Phosphorylation of (rat) BimEL at Ser-109 and Thr-110, which are adjacent to but distinct from the phosphorylation residues in 293 cells exposed to UV as mentioned above, was reported to suppress the proapoptotic function of BimEL without affecting its binding potential to LC8 or its subcellular localization (5). Fourth, proteasome-dependent degradation is involved in the regulation of Bim expression in serum-deprived fibroblasts and macrophage colony-stimulating factor-dependent osteoclasts (2, 31). These somewhat confusing results suggest that the functions of BimEL and BimL on the one hand and BimS on the other may be regulated in different ways in certain situations and that the relative importance of these four mechanisms may differ between cell types. Indeed, it has been found that the enforced expression of either BimL or BimS readily induced apoptosis in Baf-3 and 293 cells, in contrast with five glioma cell lines, in which a massive amount of BimL did not induce apoptosis, in spite of the fact that a much lower amount of BimS easily killed these cells (44, 50).

In this paper, we demonstrated that Bim is downregulated at both the mRNA and protein levels by cytokines in hematopoietic progenitors isolated from primary cultures of bone marrow cells (Fig. 2). This finding indicates that the regulation of mRNA expression is the major mechanism for controlling Bim function in early hematopoiesis. We also demonstrated that Bcr-Abl reverses the induction of Bim mRNA caused by cytokine deprivation in these progenitors (Fig. 7). Among several pathways that are reported to regulate Bim mRNA, those involved in PI3-K are most likely the major pathways for the downregulation of Bim by Bcr-Abl (Fig. 3F). In addition, phosphorylation of Bim (as with the third mechanism mentioned in the previous paragraph) might contribute to the survival of hematopoietic cells. It was previously reported that BimEL and BimL are phosphorylated in Baf-3 cells by IL-3 signaling via the same pathways that control the expression of Bim, i.e., the Ras/Raf/MAPK and Ras/PI3-K pathways (44). In this study, although the phosphorylation of BimEL in early progenitors may not be convincing (Fig. 2B), it was clearly detected in Baf-3 cells expressing Bcr-Abl cultured in IL-3-free medium and in cell lines established from patients in CML/BC cultured in the absence of imatinib (Fig. 3C). We consider it unlikely that phosphorylation plays a major role in cytokine-deprived Baf-3 cells, because cells expressing hyperphosphorylated BimEL or BimL in the presence of IL-3 still underwent apoptosis (44). However, the possibility that phosphorylation of BimEL and BimL by cytokines or Bcr-Abl contributes to cell survival to some extent in early hematopoietic progenitors or leukemic cells cannot be excluded.

There are substantial differences between early (Sca-1$^+$ c-Kit$^+$ Lin$^-$) and late (Sca-1$^-$ c-Kit$^+$ Lin$^-$) progenitors in cytokine dependence and the effects of Bcr-Abl kinase. Early progenitors undergo rapid apoptosis without maturation in the

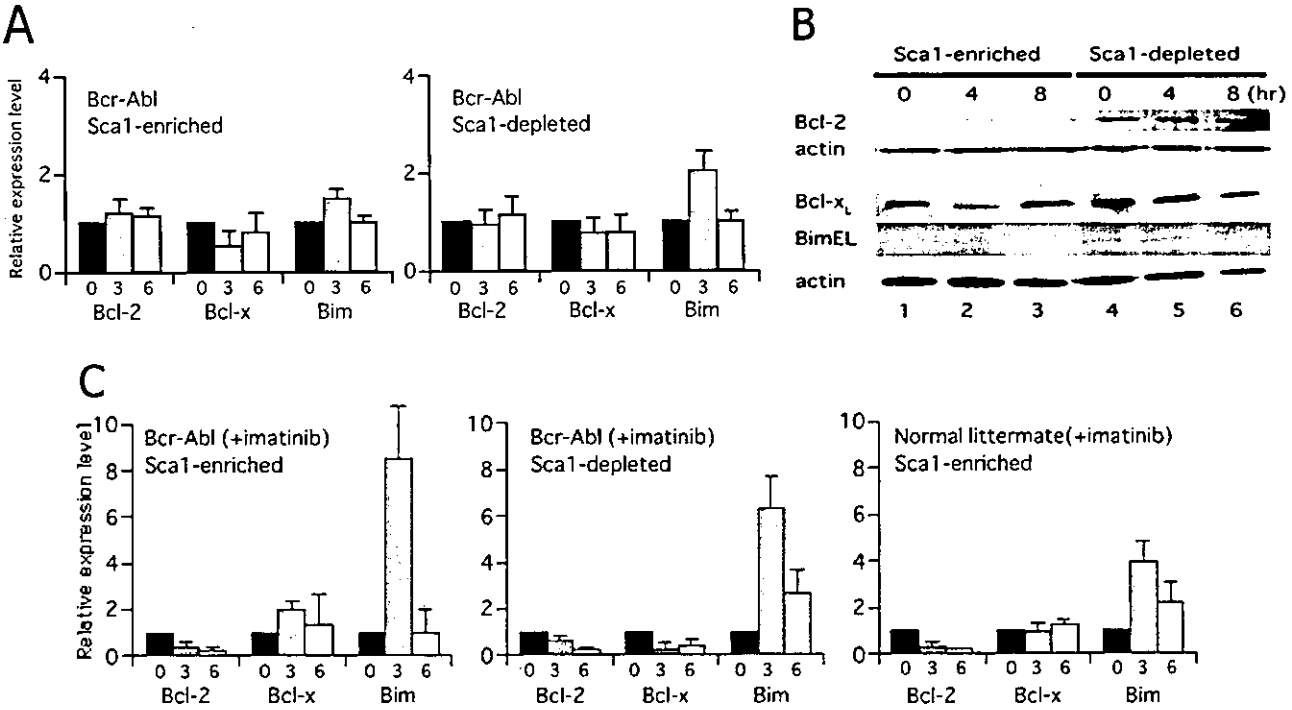

FIG. 7. Expression of Bcl-2, Bcl-x_L, and BimEL in Sca-1$^+$ c-Kit$^+$ Lin$^-$ and Sca-1$^-$ c-Kit$^+$ Lin$^-$ cells from Bcr-Abl tg mice and their normal littermates. Cells were cultured in cytokine-free medium in the absence (A and B) or presence (C) of imatinib at a concentration of 1 μM for the indicated times. (A and C) Real-time quantitative PCR was carried out, and the numbers of cycles required to produce a detectable product were measured and used to calculate the differences (*n*-fold) in starting mRNA levels for each sample by using 28S rRNA as an internal control. Levels of mRNA in cells cultured for 0 (black bars), 3 (gray bars), and 6 (open bars) h without cytokines relative to those in cells in the presence of cytokines are shown. (B) Levels of three Bcl-2 superfamily members, as well as β-actin proteins, as a control for equal loading were detected by specific antibodies.

absence of cytokines (Fig. 1C). This could be explained at least partially by relatively low levels of Bcl-2 and Bcl-x_L expression (Fig. 2B), because it is generally accepted that cell fate is determined by the balance between pro- and antiapoptotic members of the Bcl-2 superfamily (1). Although Bcl-2 levels were downregulated by cytokine deprivation in early progenitors, this downregulation is unlikely to be the major cause of rapid apoptosis, because levels of Bcl-2 in the presence of cytokines are very low and Bcl-2-deficient mice did not show apparent abnormalities in myeloid hematopoiesis (34, 47). Thus, Bim is considered to be the major determinant of cell fate in Sca-1$^+$ c-Kit$^+$ Lin$^-$ cells, and downregulation of Bim in cytokine-deprived Sca-1-positive early progenitors isolated from Bcr-Abl tg mice may result in longer survival (Fig. 6B). On the other hand, Bim may not be the major determinant of cell fate in Sca-1$^-$ c-Kit$^+$ Lin$^-$ cells, which express Bcl-2 and Bcl-x_L at high levels (Fig. 2B). Moreover, half of these cells can differentiate before undergoing apoptosis (Fig. 1C). Additionally, late progenitors from the tg mice show virtually the same time course as those from normal littermates in the absence of cytokines (Fig. 1C and 6B, right panels) in spite of the fact that there was little induction of Bim in these cells, similar to Sca-1-positive early progenitors (Fig. 7A and B).

Many reports have maintained that the growth and survival characteristics of CML progenitors in the chronic phase are similar to those in healthy bone marrow (reviewed in references 15 and 23). In spite of prominent antiapoptotic effects of Bcr-Abl in cytokine-dependent cell lines such as Baf-3, resistance of CML progenitors to cytokine deprivation is controversial. Bedi et al. reported that CD34-positive CML progenitors live longer in serum- and cytokine-free medium than CML progenitors treated with Bcr-Abl junction-specific antisense oligonucleotides and normal CD34-positive cells (4), but Amos et al. did not observe a survival advantage of CML progenitors under cytokine-free conditions (3). In the present study, we isolated early hematopoietic progenitors by using Sca-1, which is one of the most reliable markers for early progenitors, including stem cells, but is available only for the study of mouse hematopoiesis. Another advantage of our study is the use of progenitors isolated from young mice (8 to 12 weeks of age) whose peripheral blood and bone marrow are still indistinguishable from those of their normal littermates (18). Taking these advantages, we revealed a relatively small but distinct difference in apoptosis due to cytokine deprivation between normal and Bcr-Abl-expressing progenitors that correlated to the expression levels of Bim (Fig. 1, 2, 6, and 7). Moreover, Bim was induced by imatinib in CML cell lines undergoing apoptosis (Fig. 5C), and siRNA that reduced the expression level of Bim effectively rescued these cells (Fig. 5E). Taken together, these results suggest that Bim is an important downstream target that supports cell survival of Bcr-Abl-expressing hematopoietic cells. Further studies are necessary to clarify whether downregulation of Bim by Bcr-Abl contributes to the massive expansion of myeloid cells observed in CML.

ACKNOWLEDGMENTS

This work was supported in part by Grants-in-Aid for Scientific Research from the Ministry of Education, Culture, Sports, Science and Technology of Japan; the Novartis Foundation (Japan) for the promotion of Science; the Yamanouchi Foundation for Research on Metabolic Disorders; the Takeda Science Foundation; the Naito Foundation; the Uehara Memorial Foundation; the Sagawa Foundation for Promotion of Cancer Research; and the Princess Takamatsu Cancer Research Fund.

REFERENCES

1. **Adams, J. M., and S. Cory.** 1998. The Bcl-2 protein family: arbiters of cell survival. Science **281**:1322–1326.
2. **Akiyama, T., P. Bouillet, T. Miyazaki, Y. Kadono, H. Chikuda, U. I. Chung, A. Fukuda, A. Hikita, H. Seto, T. Okada, T. Inaba, A. Sanjay, R. Baron, H. Kawaguchi, H. Oda, K. Nakamura, A. Strasser, and S. Tanaka.** 2003. Regulation of osteoclast apoptosis by ubiquitylation of proapoptotic BH3-only Bcl-2 family member Bim. EMBO J. **22**:6653–6664.
3. **Amos, T. A., J. L. Lewis, F. H. Grand, R. P. Gooding, J. M. Goldman, and M. Y. Gordon.** 1995. Apoptosis in chronic myeloid leukaemia: normal responses by progenitor cells to growth factor deprivation, X-irradiation and glucocorticoids. Br. J. Haematol. **91**:387–393.
4. **Bedi, A., B. A. Zehnbauer, J. P. Barber, S. J. Sharkis, and R. J. Jones.** 1994. Inhibition of apoptosis by BCR-ABL in chronic myeloid leukemia. Blood **83**:2038–2044.
5. **Biswas, S. C., and L. A. Greene.** 2002. Nerve growth factor (NGF) down-regulates the Bcl-2 homology 3 (BH3) domain-only protein Bim and suppresses its proapoptotic activity by phosphorylation. J. Biol. Chem. **277**: 49511–49516.
6. **Bouillet, P., D. Metcalf, D. C. S. Huang, D. M. Tarlinton, T. W. H. Kay, F. Koentgen, J. M. Adams, and A. Strasser.** 1999. Proapoptotic Bcl-2 relative Bim required for certain apoptotic responses, leukocyte homeostasis, and to preclude autoimmunity. Science **286**:1735–1738.
7. **Chao, D. T., and S. J. Korsmeyer.** 1998. BCL-2 family: regulators of cell death. Annu. Rev. Immunol. **16**:395–419.
8. **Cortez, D., L. Kadlec, and A. M. Pendergast.** 1995. Structural and signaling requirements for BCR-ABL-mediated transformation and inhibition of apoptosis. Mol. Cell. Biol. **15**:5531–5541.
9. **Cortez, D., G. Stoica, J. H. Pierce, and A. M. Pendergast.** 1996. The BCR-ABL tyrosine kinase inhibits apoptosis by activating a Ras-dependent signaling pathway. Oncogene **13**:2589–2594.
10. **Crépieux, P., H. Kwon, N. Leclerc, W. Spencer, S. Richard, R. Lin, and J. Hiscott.** 1997. IκBα physically interacts with a cytoskeleton-associated protein through its signal response domain. Mol. Cell. Biol. **17**:7375–7385.
11. **Daley, G. Q., and D. Baltimore.** 1988. Transformation of an interleukin 3-dependent hematopoietic cell line by the chronic myelogenous leukemia-specific P210bcr/abl protein. Proc. Natl. Acad. Sci. USA **85**:9312–9316.
12. **Deininger, M. W., J. M. Goldman, N. Lydon, and J. V. Melo.** 1997. The tyrosine kinase inhibitor CGP57148B selectively inhibits the growth of BCR-ABL-positive cells. Blood **90**:3691–3698.
13. **Dijkers, P. F., R. H. Medema, J.-W. J. Lammers, L. Koenderman, and P. J. Coffer.** 2000. Expression of the pro-apoptotic Bcl-2 family member Bim is regulated by the forkhead transcription factor FKHR-L1. Curr. Biol. **10**: 1201–1204.
14. **Dumon, S., S. C. Santos, F. Debierre-Grockiego, V. Gouilleux-Gruart, L. Cocault, C. Boucheron, P. S Mollat, S. Gisselbrecht, and F. Gouilleux.** 1999. IL-3 dependent regulation of Bcl-x_L gene expression by STAT5 in a bone marrow derived cell line. Oncogene **18**:4191–4199.
15. **Holyoake, D. T.** 2001. Recent advances in the molecular and cellular biology of chronic myeloid leukaemia: lessons to be learned from the laboratory. Br. J. Haematol. **113**:11–23.
16. **Honda, H., Y. Yamashita, K. Ozawa, and H. Mano.** 1996. Cloning and characterization of mouse tec promoter. Biochem. Biophys. Res. Commun. **223**:422–426.
17. **Honda, H., K. Ozawa, Y. Yazaki, and H. Hirai.** 1997. Identification of PU.1 and Sp1 as essential transcriptional factors for the promoter activity of mouse tec gene. Biochem. Biophys. Res. Commun. **234**:376–381.
18. **Honda, H., H. Oda, T. Suzuki, T. Takahashi, O. N. Witte, K. Ozawa, T. Ishikawa, Y. Yazaki, and H. Hirai.** 1998. Development of acute lymphoblastic leukemia and myeloproliferative disorder in transgenic mice expressing p210bcr/abl: a novel transgenic model for human Ph1-positive leukemias. Blood **91**:2067–2075.
19. **Honda, H., T. Ushijima, K. Wakazono, H. Oda, Y. Tanaka, S. Aizawa, T. Ishikawa, Y. Yazaki, and H. Hirai.** 2000. Acquired loss of p53 induces blastic transformation in p210(bcr/abl)-expressing hematopoietic cells: a transgenic study for blast crisis of human CML. Blood **95**:1144–1150.
20. **Hsu, S. Y., P. Lin, and A. J. Hsueh.** 1998. BOD (Bcl-2-related ovarian death gene) is an ovarian BH3 domain-containing proapoptotic Bcl-2 protein capable of dimerization with diverse antiapoptotic Bcl-2 members. Mol. Endocrinol. **12**:1432–1440.
21. **Jaffrey, S. R., and S. H. Snyder.** 1996. PIN: an associated protein inhibitor of neuronal nitric oxide synthase. Science **274**:774–777.
22. **Kabarowski, J. H., P. B. Allen, and L. M. Wiedemann.** 1994. A temperature sensitive p210 BCR-ABL mutant defines the primary consequences of BCR-ABL tyrosine kinase expression in growth factor dependent cells. EMBO J. **13**:5887–5895.
23. **Kabarowski, J. H., and O. N. Witte.** 2000. Consequences of BCR-ABL expression within the hematopoietic stem cell in chronic myeloid leukemia. Stem Cells **18**:399–408.
24. **Kawauchi, K., T. Ogasawara, M. Yasuyama, and S. Ohkawa.** 2003. Involvement of Akt kinase in the action of STI571 on chronic myelogenous leukemia cells. Blood Cells Mol. Dis. **31**:11–17.
25. **King, S. M., E. Barbarese, J. F. Dillman III, R. S. Patel-King, H. Carson, and K. K. Pfister.** 1996. Brain cytoplasmic and flagellar outer arm dyneins share a highly conserved M_r 8,000 light chain. J. Biol. Chem. **271**:19358–19366.
26. **Kinoshita, T., T. Yokota, K. Arai, and A. Miyajima.** 1995. Suppression of apoptotic death in hematopoietic cells by signaling through the IL-3/GM-CSF receptors. EMBO J. **14**:266–275.
27. **Kuribara, R., T. Kinoshita, A. Miyajima, T. Shinjyo, T. Yoshihara, T. Inukai, K. Ozawa, A. T. Look, and T. Inaba.** 1999. Two distinct interleukin-3-mediated signal pathways, Ras-NFIL3 (E4BP4) and Bcl-x_L, regulate the survival of murine pro-B lymphocytes. Mol. Cell. Biol. **19**:2754–2762.
28. **Laneuville, P., N. Heisterkamp, and J. Groffen.** 1991. Expression of the chronic myelogenous leukemia-associated p210bcr/abl oncoprotein in a murine IL-3 dependent myeloid cell line. Oncogene **6**:275–282.
29. **Lei, K., and R. J. Davis.** 2003. JNK phosphorylation of Bim-related members of the Bcl2 family induces Bax-dependent apoptosis. Proc. Natl. Acad. Sci. USA **100**:2432–2437.
30. **Leverrier, Y., J. Thomas, G. R. Perkins, M. Mangeney, M. K. L. Collins, and J. Marvel.** 1997. In bone marrow derived Baf-3 cells, inhibition of apoptosis by IL-3 is mediated by two independent pathways. Oncogene **14**:425–430.
31. **Ley, R., K. Balmanno, K. Hadfield, C. R. Weston, and S. J. Cook.** 2003. Activation of the ERK1/2 signaling pathway promotes phosphorylation and proteasome-dependent degradation of the BH3-only protein, Bim. J. Biol. Chem. **278**:18811–18816.
32. **Mandanas, R. A., H. S. Boswell, L. Lu, and D. Leibowitz.** 1992. BCR/ABL confers growth factor independence upon a murine myeloid cell line. Leukemia **6**:796–800.
33. **Mano, H., F. Ishikawa, J. Nishida, H. Hirai, and F. Takaku.** 1990. A novel protein-tyrosine kinase, tec, is preferentially expressed in liver. Oncogene **5**:1781–1786.
34. **Matsuzaki, Y., K. Nakayama, K. Nakayama, T. Tomita, M. Isoda, D. Y. Loh, and H. Nakauchi.** 1997. Role of bcl-2 in the development of lymphoid cells from the hematopoietic stem cell. Blood **89**:853–862.
35. **Miyajima, A., Y. Ito, and T. Kinoshita.** 1999. Cytokine signaling for proliferation, survival, and death in hematopoietic cells. Int. J. Hematol. **69**:137–146.
36. **O'Connor, L., A. Strasser, L. A. O'Reilly, G. Hausmann, J. M. Adams, S. Cory, and D. C. Huang.** 1998. Bim: a novel member of the Bcl-2 family that promotes apoptosis. EMBO J. **17**:384–395.
37. **Okabe, M., Y. Uehara, T. Miyagishima, T. Itaya, M. Tanaka, Y. Kuni-Eda, M. Kurosawa, and T. Miyazaki.** 1992. Effect of herbimycin A, an antagonist of tyrosine kinase, on bcr/abl oncoprotein-associated cell proliferations: abrogative effect on the transformation of murine hematopoietic cells by transfection of a retroviral vector expressing oncoprotein P210bcr/abl and preferential inhibition on Ph1-positive leukemia cell growth. Blood **80**:1330–1338.
38. **Onishi, M., S. Kinoshita, Y. Morikawa, A. Shibuya, J. Phillips, L. L. Lanier, D. M. Gorman, G. P. Nolan, A. Miyajima, and T. Kitamura.** 1996. Application of retrovirus-mediated expression cloning. Exp. Hematol. **24**:324–329.
39. **Packham, G., E. L. White, C. M. Eischen, H. Yang, E. Parganas, J. N. Ihle, D. A. Grillot, G. P. Zambetti, G. Nunez, and J. L. Cleveland.** 1998. Selective regulation of Bcl-XL by a Jak kinase-dependent pathway is bypassed in murine hematopoietic malignancies. Genes Dev. **12**:2475–2487.
40. **Putcha, G. V., K. L. Moulder, J. P. Golden, P. Bouillet, J. A. Adams, A. Strasser, and E. M. Johnson.** 2001. Induction of BIM, a proapoptotic BH3-only BCL-2 family member, is critical for neuronal apoptosis. Neuron **29**: 615–628.
41. **Puthalakath, H., D. C. Huang, L. A. O'Reilly, S. M. King, and A. Strasser.** 1999. The proapoptotic activity of the Bcl-2 family member Bim is regulated by interaction with the dynein motor complex. Mol. Cell **3**:287–296.
42. **Reginato, M. J., K. R. Mills, J. K. Paulus, D. K. Lynch, D. C. Sgroi, J. Debnath, S. K. Muthuswamy, and J. S. Brugge.** 2003. Integrins and EGFR coordinately regulate the pro-apoptotic protein Bim to prevent anoikis. Nat. Cell Biol. **5**:733–740.
43. **Schaich, M., T. Illmer, G. Seitz, B. Mohr, U. Schakel, J. F. Beck, and G. Ehninger.** 2001. The prognostic value of Bcl-x_L gene expression for remission induction is influenced by cytogenetics in adult acute myeloid leukemia. Haematologica **86**:470–477.
44. **Shinjyo, T., R. Kuribara, T. Inukai, H. Hosoi, T. Kinoshita, A. Miyajima, P. J. Houghton, A. T. Look, K. Ozawa, and T. Inaba.** 2001. Downregulation of Bim, a proapoptotic relative of Bcl-2, is a pivotal step in cytokine-initiated

survival signaling in murine hematopoietic progenitors. Mol. Cell. Biol. **21:** 854–864.

45. **Silva, M., A. Benito, C. Sanz, F. Prosper, D. Ekhterae, G. Nunez, and J. L. Fernandez-Luna.** 1999. Erythropoietin can induce the expression of bcl-x(L) through Stat5 in erythropoietin-dependent progenitor cell lines. J. Biol. Chem. **274:**22165–22169.
46. **Socolovsky, M., A. E. Fallon, S. Wang, C. Brugnara, and H. F. Lodish.** 1999. Fetal anemia and apoptosis of red cell progenitors in Stat5a$^{-/-}$5b$^{-/-}$ mice: a direct role for Stat5 in Bcl-X(L) induction. Cell **98:**181–191.
47. **Veis, D. J., C. M. Sorenson, J. R. Shutter, and S. J. Korsmeyer.** 1993. Bcl-2-deficient mice demonstrate fulminant lymphoid apoptosis, polycystic kidneys, and hypopigmented hair. Cell **75:**229–240.
48. **Weston, C. R., K. Balmanno, C. Chalmers, K. Hadfield, S. A. Molton, R. Ley, E. F. Wagner, and S. J. Cook.** 2003. Activation of ERK1/2 by deltaRaf-1:ER* represses Bim expression independently of the JNK or PI3K pathways. Oncogene **22:**1281–1293.
49. **Whitfield, J., S. J. Neame, L. Paquet, O. Bernard, and J. Ham.** 2001. Dominant-negative c-Jun promotes neuronal survival by reducing BIM expression and inhibiting mitochondrial cytochrome c release, Neuron **29:**629–643.
50. **Yamaguchi, T., T. Okada, T. Takeuchi, T. Tonda, M. Ohtaki, S. Shinoda, T. Masuzawa, K. Ozawa, and T. Inaba.** 2003. Enhancement of thymidine kinase-mediated killing of malignant glioma by BimS, a BH3-only cell death activator. Gene Ther. **10:**375–385.

THE JOURNAL OF GENE MEDICINE
J Gene Med 2004; 6: 1049–1060.
Published online 1 June 2004 in Wiley InterScience (www.interscience.wiley.com). DOI: 10.1002/jgm.609

RESEARCH ARTICLE

Sustained transgene expression by human cord blood derived CD34$^+$ cells transduced with simian immunodeficiency virus agmTYO1-based vectors carrying the human coagulation factor VIII gene in NOD/SCID mice

Jiro Kikuchi[1]
Jun Mimuro[1,2]*
Kyoichi Ogata[1]
Toshiaki Tabata[3]
Yasuji Ueda[3]
Akira Ishiwata[1]
Konzoh Kimura[1]
Katsuhiro Takano[1]
Seiji Madoiwa[1,2]
Hiroaki Mizukami[4]
Yutaka Hanazono[4]
Akihiro Kume[4]
Mamoru Hasegawa[3]
Keiya Ozawa[2,4]
Yoichi Sakata[1,2]

[1]*Division of Cell and Molecular Medicine, The Center for Molecular Medicine, Jichi Medical School, Tochigi-ken 329-0498, Japan*

[2]*Hematology Division of Department of Medicine, Jichi Medical School, Tochigi-ken 329-0498, Japan*

[3]*DNAVEC Research Inc., Ibaraki-ken 305-0003, Japan*

[4]*Division of Genetic Therapeutics, The Center for Molecular Medicine, Jichi Medical School, Tochigi-ken 329-0498, Japan*

*Correspondence to: Jun Mimuro, Division of Cell and Molecular Medicine, Center for Molecular Medicine, Jichi Medical School, Tochigi-ken 329-0498, Japan.
E-mail: mimuro-j@jichi.ac.jp

Received: 16 September 2003
Revised: 12 February 2004
Accepted: 22 March 2004

Abstract

Background Gene therapy is being studied as the next generation therapy for hemophilia and several clinical trials have been carried out, albeit with limited success. To explore the possibility of utilizing autologous bone marrow transplantation of genetically modified hematopoietic stem cells for hemophilia gene therapy, we investigated the efficacy of genetically engineered CD34$^+$ cell transplantation to NOD/SCID mice for expression of human factor VIII (hFVIII).

Methods CD34$^+$ cells were transduced with a simian immunodeficiency virus agmTYO1 (SIV)-based lentiviral vector carrying the enhanced green fluorescent protein (eGFP) gene (SIVeGFP) or the hFVIII gene (SIVhFVIII). CD34$^+$ cells transduced with SIV vectors were transplanted to NOD/SCID mice. Engraftment of transduced CD34$^+$ cells and expression of transgenes were studied.

Results We could efficiently transduce CD34$^+$ cells using the SIVeGFP vector in a dose-dependent manner, reaching a maximum ($99.6 \pm 0.1\%$) at MOI of 5×10^3 vector genome/cell. After transducing CD34$^+$ cells with SIVhFVIII, hFVIII was produced (274.3 ± 20.1 ng) from 10^6 CD34$^+$ cells during 24 h *in vitro* incubation. Transplantation of SIVhFVIII-transduced CD34$^+$ cells ($5–10 \times 10^5$) at a multiplicity of infection (MOI) of 50 vector genome/cell into NOD/SCID mice resulted in successful engraftment of CD34$^+$ cells and production of hFVIII (minimum 1.2 ± 0.9 ng/mL, maximum 3.6 ± 0.8 ng/mL) for at least 60 days *in vivo*. Transcripts of the hFVIII gene and the hFVIII antigen were also detected in the murine bone marrow cells.

Conclusions Transplantation of *ex vivo* transduced hematopoietic stem cells by non-pathogenic SIVhFVIII without exposure of subjects to viral vectors is safe and potentially applicable for gene therapy of hemophilia A patients.

Keywords hemophilia; gene therapy; simian immunodeficiency virus; hematopoietic stem cell

Introduction

Hemophilia A is an inherited X-linked lifelong bleeding disorder caused by abnormality in the coagulation factor VIII (FVIII) gene [1]. The genetic abnormalities result in deficiency of FVIII, which in turn creates a bleeding

phenotype, such as life-threatening intracranial bleeding and bleeding in joints and muscles. Hemophilias occur as mild, moderate, or severe phenotypes, depending on the blood FVIII level of 6% or more, 2–5%, or 1% or less [1,2]. Current standard therapy is intravenous (i.v.) injection of human plasma-derived FVIII or recombinant FVIII. Aside from certain specific situations such as pre-operative factor coverage, i.v. infusion of FVIII usually is used to treat acute bleeding episodes. However, maintenance of blood FVIII levels to more than 5% of the normal FVIII concentration may result in significant clinical improvement. Furthermore, if one can increase FVIII levels to more than 1% in severe hemophilia patients, they may have significantly fewer bleeding episodes and improved quality of life. Additionally, in the past, infection with hepatitis B and C viruses or human immunodeficiency virus (HIV) in hemophilia patients was a tragic result of contaminated blood-derived commercial products. In this regard, gene therapy is being explored as the next generation therapy for hemophilia patients. Hemophilia is considered suitable for gene therapy for the following reasons: (1) treatment is feasible through replacement of a normal copy of the factor VIII gene; (2) increase of factor VIII levels to just 1% or more of the normal level may provide significant clinical improvement; and (3) gene therapy offers the potential for more sustained and less expensive treatment than the current standard therapy [2].

Hematopoietic stem cells are thought to be highly desirable targets for gene therapy because of their capability for self-renewal and multi-lineage differentiation [3]. Non-obese diabetic severe combined immunodeficient (NOD/SCID) mice are well-characterized immunodeficient mice obtained by transferring the SCID mutation onto the NOD background. They lack functional T and B cells and diminished natural killer (NK) and macrophage activities and, thus, they are thought to be suited for transplantation of hematopoietic stem cells. Human hematopoietic stem cells can be engrafted and generate their progeny in NOD/SCID mice, and virally transduced hematopoietic stem cells have also been transplanted successfully into NOD/SCID mice [4–6].

Retroviral vectors including lentiviral vectors are now widely used to transduce hematopoietic stem cells [4–6]. These vectors can integrate transgenes into the target cell genome, allowing transmission of the transgenes to daughter cells *in vivo* [7]. Lentiviral vectors transduce hematopoietic stem cells more efficiently than the classical retroviral vectors. However, there are safety concerns in utilizing HIV-1-based lentiviral vectors for gene therapy clinical trials. In this regard, simian immunodeficiency virus agmTYO1 (SIVagmTYO1)-based vectors are of particular interest. SIVagmTYO1 is an HIV-related lentivirus isolated from the African green monkey and shown to be non-pathogenic to both their natural hosts and to experimentally inoculated Asian macaques [8,9]. Additionally, due to the use of contaminated blood products, some hemophilia patients are HIV-1 carriers. If an HIV-1-based vector is administrated to such patients, the replication-competent lentivirus particles carrying the therapeutic gene may be generated by homologous recombination between the recombinant HIV vector and the wild-type HIV genome. The packaging signal in the HIV vector sequence may be another factor contributing to production of replication-competent lentivirus particles. From this perspective, then, a SIV vector based on the SIVagmTYO1 strain may be a better vehicle for hemophilia gene therapy because SIVagmTYO1 has less than 60% genomic sequence similarity to HIV-1. We have developed SIVagmTYO1-based vectors that can transduce various cells, including hematopoietic stem cells. While early studies have indicated the lack of factor VIII secretion by hematopoietic cells [10], recent studies have shown the ability of hematopoietic cell lines [11] and stem cells [12,13] to secrete detectable amounts of factor VIII upon lentiviral transduction. In the present study, we use human cord blood derived $CD34^+$ (CB-$CD34^+$) cells and SIVagmTYO1-based vectors to show that high FVIII expression levels are achieved in $CD34^+$ cells transduced with the SIV vector *in vitro* and that transplantation of SIVagmTYO1 vector-transduced hematopoietic stem cells may be used for hemophilia gene therapy *in vivo*.

Materials and methods

Cell lines, medias and cytokines

Recombinant human thrombopoietin (TPO) and stem cell factor (SCF) were kindly supplied by Kirin Brewery Co. (Tokyo, Japan). Dulbecco's modified Eagle's medium (DMEM) and Iscove's modified Dulbecco's medium (IMDM) were purchased from Invitrogen Japan (Tokyo, Japan) and fetal bovine serum (FBS) from Hyclone (Logan, UT, USA). Human embryonal kidney 293T (HEK293T) cells were obtained from the American Type Culture Collection (Manassas, VA, USA) and cultured in DMEM containing 10% FBS.

$CD34^+$ cell purification

Cord blood was drawn from umbilical cords of normal full-term deliveries after obtaining informed consent. Mononuclear cells were separated by density gradient centrifugation using Lymphoprep tubes (Dai-ichi Pharmaceutical, Tokyo, Japan) after depletion of phagocytes using silica particles (Immuno Biological Laboratories, Gunma, Japan). The mononuclear cells were suspended in phosphate-buffered saline (PBS) at $3–5 \times 10^7$ cells/ml and mixed with Dynabeads M-450 CD34 (Dynal AS, Oslo, Norway) at a bead-to-cell ratio of 1 : 1. After incubation at 4 °C for 30 min with gentle rotation, the cell-beads suspension was placed in a DYNAL MPC (magnetic particle concentrator) to collect the Dynabeads M-450 CD34-rosetted cells. The rosetted cells were incubated with DETACHaBEAD CD34 (Dynal) at 37 °C for 15 min to release $CD34^+$ cells from the beads. The purity of $CD34^+$

cells was evaluated by flow cytometry using a FACScan (Becton Dickinson) and approximately 95% of the separated cells were CD34-positive.

Production of SIVagm vectors

Human FVIII cDNA spanning the entire coding region was a generous gift from Dr. J. A. van Mourik. Because the B domain is excised from other FVIII domains upon activation by thrombin and is not essential for coagulation activity expression of FVIIIa, the human FVIII cDNA was subjected to PCR-based mutagenesis to delete most of the fragment that encodes the FVIII B domain (BDD FVIII cDNA) as described previously [14]. The characteristics and production of SIVagm vector used in this study have been described previously [9,14]. Self-inactivating SIVagm vectors are pseudotyped with vesicular stomatitis virus glycoprotein G (VSVG). We constructed gene transfer vectors to express the hBDDFVIII gene and eGFP gene driven by the cytomegalovirus (CMV) promoter. To produce SIV vectors, HEK293T cells were transfected with the packaging vector, the gene transfer vector, and pVSVG (Clontech) as described previously [9,14]. Transduction units of SIV vectors carrying the eGFP gene (SIVeGFP) were determined by infection of SIVeGFP to HEK293T cells followed by determination of eGFP expression by FACS analysis. Since determination of transduction units of SIV vectors carrying the human BDDFVIII cDNA (SIV hFVIII) was difficult compared with SIV eGFP, RNA dot blot analysis was performed to quantify the amount of SIV vector genome (vg) of vector preparations. To detect replication-competent SIV particles in cells infected with SIV vectors, HEK 293T cells were cultivated in media containing SIV eGFP or SIV hVIII at a multiplicity of infection (MOI) of 100 vg/cell. RNA was isolated from the supernatants of vector-infected cells on day 6 after infection using an RNA isolation kit (QIAamp viral RNA mini kit; QIAGEN). Detection of the gag gene and the pol gene required for virus replication in the RNA preparation was carried out by reverse transcription-polymerase chain reaction (RT-PCR) using the gag-specific primers (5′-GTC CTA GAC ATT AGG CAG GGA CCT-3′, 5′-TTT TGC CCC CAT CCA CCG TCC ATA-3′) and the pol-specific primers (5′-CAG AAA TTC AAA AGA AGG AAA AGC A-3′, 5′-CTT CTT GGG AGG TAA AGT TAG GCC CA-3′), respectively.

In vitro culture and transduction of human CB-CD34$^+$ cells

The cells were cultivated at 5×10^5 cells/mL in IMDM supplemented with 1% bovine serum albumin (BSA), 10 μg/mL bovine pancreatic insulin, 200 μg/mL human transferrin (BIT 9500; StemCell Technologies, Vancouver, Canada), 40 μg/mL human low-density lipoproteins (Chemicon International), 10^{-4} mol/L 2-mercaptoethanol, SCF (100 ng/mL) and TPO (50 ng/mL) at 37 °C with 5% CO_2 in 48-well tissue culture plates (Falcon, Lincoln Park, NJ, USA) [15]. For transduction, SIV vector ($0.25–5 \times 10^{10}$ vg/mL) was added to the cell suspension, and the plates were incubated at 37 °C in the presence of 5% CO_2. After incubation, SIVeGFP-transduced CD34$^+$ cells were analyzed for eGFP expression by flow cytometry and the conditioned medium of SIVhFVIII-transduced CD34$^+$ cells was harvested and subjected to FVIII enzyme-linked immunosorbent assay (ELISA).

Mice

Experimental NOD/SCID mice were obtained from the Central Institute for Experimental Animals (Kawasaki, Japan). The NOD/SCID mice were kept in a clean experimental room and were maintained on a γ-irradiated sterile diet and given autoclaved, distilled water containing 1 μg/mL of neomycin sulfate after transplantation [16]. Peripheral blood was drawn into EDTA-containing tubes from mouse tail veins and platelet-poor plasma was prepared by centrifugation. Platelet-rich plasma was also prepared from 1 mL of mouse blood upon sacrifice. Platelets were collected from platelet-rich plasma by centrifugation and were extracted in 50 μL of 0.5% Triton X-100/PBS. Bone marrow cells and bone marrow blood were collected from femurs by irrigation with PBS. After centrifugation, bone marrow cells were subjected to fluorescence-activated cell sorting (FACS) analyses and the supernatants were subjected to ELISA for quantification of human FVIII. The bone marrow volume of a mouse femur preparation was estimated to 10 mm^3 since it was approximately one-third of the volume of the femur calculated by the expression of 1 mm (radius)$^2 \times \pi \times 10$ mm (length).

Transplantation of CB-CD34$^+$ cells into NOD/SCID mice

Xenograft transplantation of the CB-CD34$^+$ cells was performed according to methods previously described [16]. Briefly, $5–10 \times 10^5$ CB-CD34$^+$ cells were transduced with SIVagm vector and injected into 6- to 12-week-old NOD/SCID mice through the tail vein after sub-lethal irradiation with 350–360 cGy of γ-ray (^{60}Co, Gamma Cell; Nortion International, Kanata, ON, Canada). For internal controls, NOD/SCID mice were injected with non-transduced (mock) CB-CD34$^+$ cells using identical procedures. Because NK cell activity of NOD/SCID mice is not completely impaired, 400 μL of PBS containing 20 μL of anti-asialo GM1 antiserum (Wako; Osaka, Japan) were injected intraperitoneously to the recipient mice immediately before the cell transplantation to delete NK cells [17]. Anti-asialo GM1 antiserum injection was carried out once a week after transplantation of CD34$^+$ cells. Peripheral blood (100 μL) was collected from mouse tail veins into tubes containing EDTA. Platelet-rich plasma (PRP) was prepared by centrifuging whole blood at 200 *g*

for 10 min. After collection of PRP, platelet-poor plasma was prepared by centrifugation at 400 *g* for 5 min, and subjected to FVIII ELISA. Peripheral leukocytes were prepared after disrupting red blood cells using Lysis buffer (155 mM NH_4Cl, 10 mM NH_4HCO_3, 0.1 mM EDTA, pH 7.4). Leukocytes and platelets were subjected to flow cytometric analysis using the FACScan. Mice were sacrificed on day 60 after transplantation. Bone marrow cells were drawn from femurs and the spleen cells were also collected. These cell suspensions were filtered through sterile 40-μm cell strainers (#2340; Falcon) to get rid of clumps and clots [16]. Cells and platelets were processed for flow cytometric analysis and the immunofluorescent analysis (see below). Platelet-poor plasma prepared from peripheral blood and the supernatant of bone marrow cell suspension were subjected to the FVIII ELISA assay.

Flow cytometric analysis of transplanted human cells in NOD/SCID mice

Surface markers on human hematopoietic cells reconstituted in peripheral blood, bone marrow cells, and spleen cells of NOD/SCID mice were analyzed by flow cytometry as described [18]. Briefly, after depletion of erythrocytes using Lysis buffer, mouse peripheral white blood cells, bone marrow cells, spleen cells, and platelets were incubated on ice for 30 min with a series of fluorescence-labeled monoclonal antibodies (Dako Japan, Tokyo, Japan) to human cluster of differentiation (CD) antigens in 100 μL of PBS containing 5% FBS. The presence of human hematopoietic cells was determined by detection of cells positively stained with phycoerythrin-cyanine 5-succinimidyl ester (PE-Cy5)-conjugated anti-human CD45. Successful engraftment of human hematopoietic cells was defined by the presence of at least 1% of human $CD45^+$ cells in peripheral blood or bone marrow of NOD/SCID mouse 60 days after transplantation [17,18]. Specific subsets of human hematopoietic cells were quantified by gating human CD45-positive cells and detection of surface antigens with fluorescein isothiocyanate isomer-1 (FITC)-conjugated anti-human CD3 and CD33 or R-phycoerythrin(RPE)-conjugated anti-human CD14, CD19, and CD34. Platelets, separated from the peripheral blood or the bone marrow, were detected with RPE-conjugated anti-human CD41.

ELISA for hFVIII antigen

Since human FVIII (hFVIII) clotting activity could not be quantified directly in the NOD/SCID mice because of the presence of endogenous murine FVIII in the plasma, hFVIII expressed in NOD/SCID mice was quantified by a hFVIII-specific ELISA as described previously [14,19]. Briefly, 96-well microtiter plates (Costar, Cambridge, MA, USA) were coated with 1 μg/mL mouse monoclonal antibodies to hFVIII (Chemo-Sero Therapeutic Institute, Kumamoto, Japan) [19]. After blocking with 5% casein in PBS, mouse plasma samples or pooled normal human plasma in Tris-buffered saline (TBS) containing 0.1% Tween 20, 1% casein were added. After 16 h incubation at 4 °C, hFVIII bound to the plates was detected with sheep anti-hFVIII polyclonal antibodies (Cedarlane Laboratories Ltd, Homby, ON, Canada) and horseradish peroxidase-conjugated rabbit anti-sheep IgG. Monoclonal antibody-purified hFVIII was kindly provided by the Chemo-Sero Therapeutic Institute and was used as the standard. Normal pooled platelet-poor plasma was also used as the standard. The ELISA could specifically detect hFVIII in mouse plasma as low as 0.5 ng/mL or FVIII in 300-fold diluted normal human plasma [14].

Immunofluorescence microscopy

Bone marrow cells were attached to glass slides using a Cytospin3 (Shandon, ThermoShandon, Inc., Pittsburgh, PA, USA), fixed with 4% paraformaldehyde in PBS and blocked with 1% BSA and 1% donkey serum in PBS. Samples were incubated with polyclonal anti-hFVIII antibody at 4 °C for 16 h. After washing in PBS, cells were incubated with donkey anti-sheep IgG antibody conjugated with Alexa488 (Molecular Probes, Eugene, OR, USA) at 4 °C for 16 h for visualization of hFVIII by fluorescent microscopy as described previously [14].

Detection of the BDD-FVIII transcript by RT-PCR

Total cellular RNA was isolated from 10^5 cells by the acid-guanidine method [20] and were reverse-transcribed to cDNA using reverse transcriptase (Superscript; Invitrogen Japan, Tokyo, Japan) and oligo-(dT) primers in a 20 μL mixture (QIAGEN Japan, Tokyo, Japan) after DNase I (Amplification grade, Invitrogen) treatment. Subsequent PCR-amplification was carried out with 1 μL of cDNA solution (corresponding to 5000 cells) in a 50 μL reaction mixture containing 5 units of Taq polymerase, 10 mmol/L Tris-HCl (pH 8.5), 50 mmol/L KCl, 1.5 mmol/L $MgCl_2$ and 100 μmol/L dNTPs in the presence of specific primer pairs (200 nmol/L) designed to amplify the DNA fragments derived from the transcript of the BDD-FVIII transgene [14]. Each PCR cycle consisted of denaturation at 94 °C for 15 s, annealing at 55 °C for 30 s, and extension at 72 °C for 30 s. The PCR products were analyzed by agarose gel electrophoresis. Authenticity of PCR products was confirmed by their molecular sizes on agarose gel electrophoresis, and their sequences. The primer sequences are as follows: hFVIII: sense, 5′-ATT GGA GCA CAG ACT GAC TT-3′; antisense, 5′-ATA TGG TAT CAT CAT AGT CA-3′ (400 bp); human GAPDH: sense, 5′-TGA TGA CAT CAA GAA GGT GGT GAA G-3′; antisense, 5′-TCC TTG GAG GCC ATG TGG GCC AT-3′ (240 bp); mouse GAPDH: sense, 5′-GCA GTG GCA AGT GGC AAA GTG GAG ATT-3′; antisense, 5′-TGA GTG GAG TCA TAC TGG AAC ATG-3′ (88 bp)

Results

SIV vectors

SIV vectors carrying the human BDDFVIII cDNA (SIVhFVIII) used in this study have been shown previously to transduce cells efficiently *in vitro* and *in vivo* [14]. No PCR-amplified fragments for the SIV gag gene or the SIV pol gene were detected by RT-PCR in the supernatants of vector-infected 293T cells *in vitro* (not shown), suggesting that no replication-competent virus particles were generated in the vector-infected cells.

Transduction of CB-CD34$^+$ cells with SIVeGFP and SIVhFVIII

To assess the *in vitro* transduction efficiency of CB-CD34$^+$ cells with the SIV vector, CB-CD34$^+$ cells were cultured in the presence of increasing concentrations of SIVeGFP for 48 h or in the presence of the fixed concentration of SIVeGFP for various incubation times. After incubation, expression of eGFP in CB-CD34$^+$ cells was analyzed by flow cytometry. As shown in Figure 1A, eGFP expression in CB-CD34$^+$ cells increased in a dose-dependent manner. 99.6 ± 0.1% of CB-CD34$^+$ cells were efficiently transduced with SIVeGFP at MOI of 5×10^3 vg/cell (100 TU/cell). Half-maximal expression of eGFP was achieved when cells were incubated with SIVeGFP at MOI of 50 vg/cell (1TU/cell). When CB-CD34$^+$ cells were cultured in the presence of SIVeGFP at MOI of 50 vg/cell (1TU/cell), expression of eGFP increased with time, reaching a maximum at 48 h incubation, followed by a gradual decline at 72 h (Figure 1B). The gradual decline in eGFP expression may be due to either pseudotransduction or reduction of cell viability. We also assessed hFVIII production in CB-CD34$^+$ cells *in vitro*. CB-CD34$^+$ cells were incubated in the presence of increasing concentrations of SIVhFVIII and the supernatants were harvested after 48 h incubation and were subjected to ELISA for the hFVIII antigen. FVIII production in the CB-CD34$^+$ cells increased in a dose-dependent manner, reaching a maximum at 274.3 ± 20.1 ng/10^6 cells/24 h at MOI of 5×10^3 vg/cell (Figure 1C).

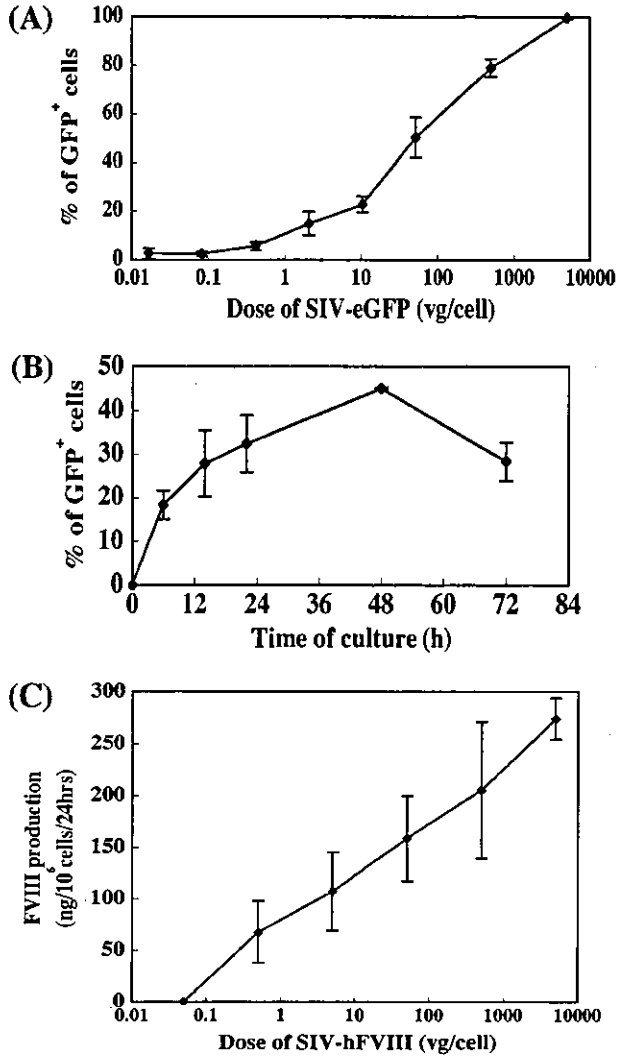

Figure 1. Transduction of CB-CD34$^+$ cells by SIVeGFP and SIVhFVIII. CB-CD34$^+$ cells (5×10^5 cells/mL) were incubated with increasing concentrations of SIVeGFP for 48 h (A) or with a fixed concentration (MOI, 50 vg/cell) of SIVeGFP for various times (B). After incubation, expression of eGFP was analyzed by flow cytometry. The percentages of transduced cells expressing eGFP are shown (mean ± SD, n = 3). CB-CD34$^+$ cells (5×10^5 cells/mL) were incubated with increasing concentrations of SIVhFVIII and supernatants were harvested after 24 h incubation and subjected to the FVIII ELISA for quantification of the hFVIII antigen (mean ± SD, n = 3)

Determination of human CB-CD34$^+$ cell-derived white blood cells in NOD/SCID mice

CB-CD34$^+$ cells were transduced with the SIVhFVIII vector in the presence of TPO and SCF, because transduction efficiency is enhanced when cells are induced to enter the cell cycle [21]. Reduced cell viability after transduction was observed due to exposure with SIV in the absence of cytokines and even in the presence of cytokines at high MOIs (data not shown). Reduction of cell viability observed during transduction may well be due to cytotoxicity of VSVG. *Ex vivo* expanded CB-CD34$^+$ cells are reportedly less potent for engraftment *in vivo* [22]. Therefore, we transduced cells with an MOI of 50 vg/cell for 24 h in the presence of cytokines and then transplanted them into NOD/SCID mice. 5×10^5 of the transduced CB-CD34$^+$ cells (+/− hFVIII) suspended in 400 μL of IMDM were injected intravenously (i.v.) into NOD/SCID mice after sub-lethal irradiation as described in Methods. Peripheral white blood cells were obtained from recipient mice and were subjected to flow cytometry to confirm engraftment of the human cells. Figure 2 shows the percentage of human CD45$^+$ cells in peripheral white blood and bone marrow cells of NOD/SCID mice after

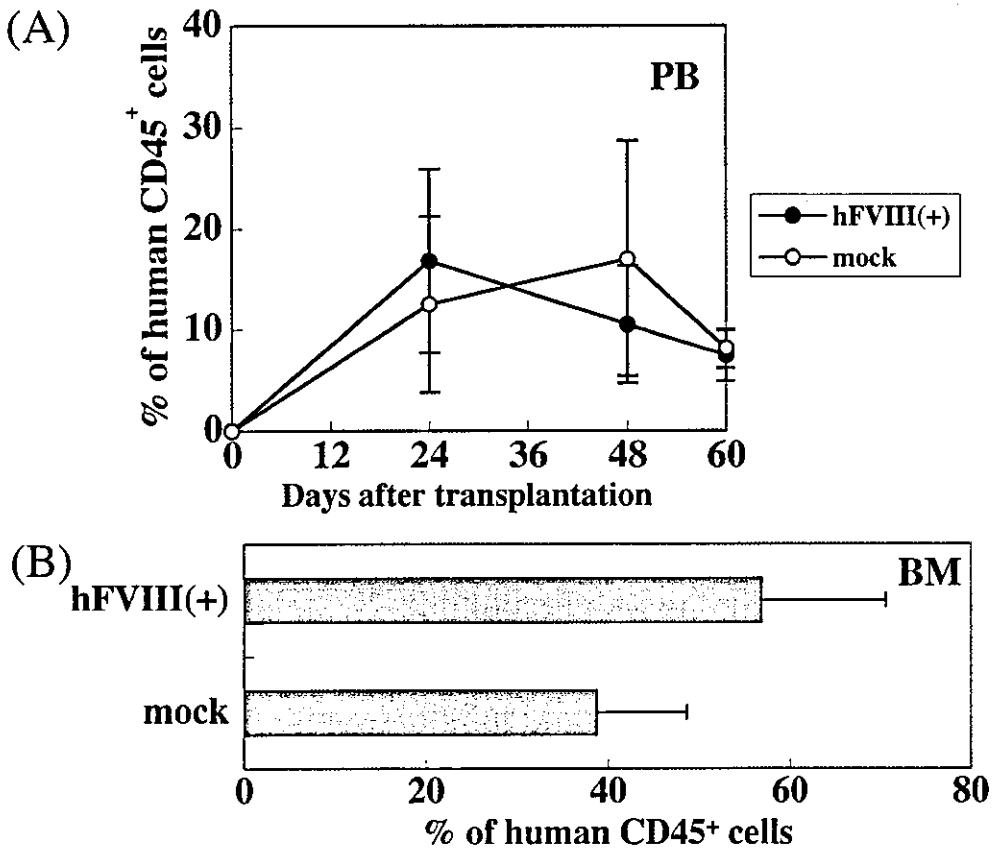

Figure 2. Presence of human CD45$^+$ cells in peripheral white blood and bone marrow cells of NOD/SCID mice after transplantation of human CB-CD34$^+$ cells. Peripheral blood was obtained from recipient mice on days 24, 48, and 60 after transplantation of CB-CD34$^+$ cells. White blood cells derived from transplanted human cells were quantified by detecting human CD45$^+$ cells by flow cytometry. The percentages of human CD45$^+$ cells in peripheral blood white blood cells (PB) from the NOD/SCID mice who received SIVhFVIII (closed circles) and mock (open circles) transduced CB-CD34$^+$ cells (A) and those in bone marrow cells (BM) collected on day 60 (B) are shown (mean ± SD, n = 3)

transplantation. The percentages of human CD45$^+$ cells in mouse peripheral white blood cells were 16.8 ± 9.1% on day 24, 10.5 ± 5.8% on day 48 and 7.4 ± 2.5% on day 60 after transplantation (Figure 2A). When the mice were sacrificed on day 60, the percentage of human CD45$^+$ cells in bone marrow cells was 56.9 ± 9.9%(Figure 2B). These data suggested that the transplanted human cells were well engrafted in the NOD/SCID mice.

Plasma hFVIII levels in NOD/SCID mice after transplantation

Mouse plasma was obtained on days 1, 6, 24, 48 and 60 after transplantation and human FVIII (hFVIII) levels in mouse plasma were quantified by the hFVIII-specific ELISA. Plasma hFVIII levels rose to 3.0 ± 1.2 ng/mL on day 1 and reached a maximum at 3.6 ± 0.8 ng/mL on day 6 after transplantation. hFVIII levels gradually decreased by 24 days, but continued a low-level basal production of at least 1.2 ng/mL for 60 days after transplantation (Figure 3A). Since the normal hFVIII concentration in human plasma is 100–200 ng/mL [23], levels of hFVIII in plasma of NOD/SCID mice which received transduced cell transplantation were approximately 1–3% of the normal hFVIII. However, hFVIII levels in the bone marrow of recipient mice were 13.4 ± 6.5 ng/mL (Figure 3B), suggesting that those in recipient mouse bone marrow were considerably higher than the plasma levels. Control animals that received mock-transduced human CB-CD34$^+$ cells did not yield any detectable hFVIII in their plasma or the bone marrow.

Expression of CD markers in engrafted human cells from peripheral blood, spleen, and bone marrow

To analyze populations of human cells in CB-CD34$^+$ cell-engrafted NOD/SCID mice, bone marrow cells and spleen cells were isolated at 60 days after transplantation and analyzed for the expression of human lineage-specific markers by flow cytometry. Figure 4 shows a typical analysis of bone marrow cells from a mouse engrafted with SIVhFVIII-transduced CB-CD34$^+$ cells. From this mouse bone marrow, 42.8% of mouse bone marrow cells were positive for human CD45. In the human CD45$^+$ cell fraction, human CD34, CD19, CD3, CD14, or CD33 positive cells were 22.9, 65.1, 0.1, 14.8, and 13.2%, respectively. On average, human CD45$^+$

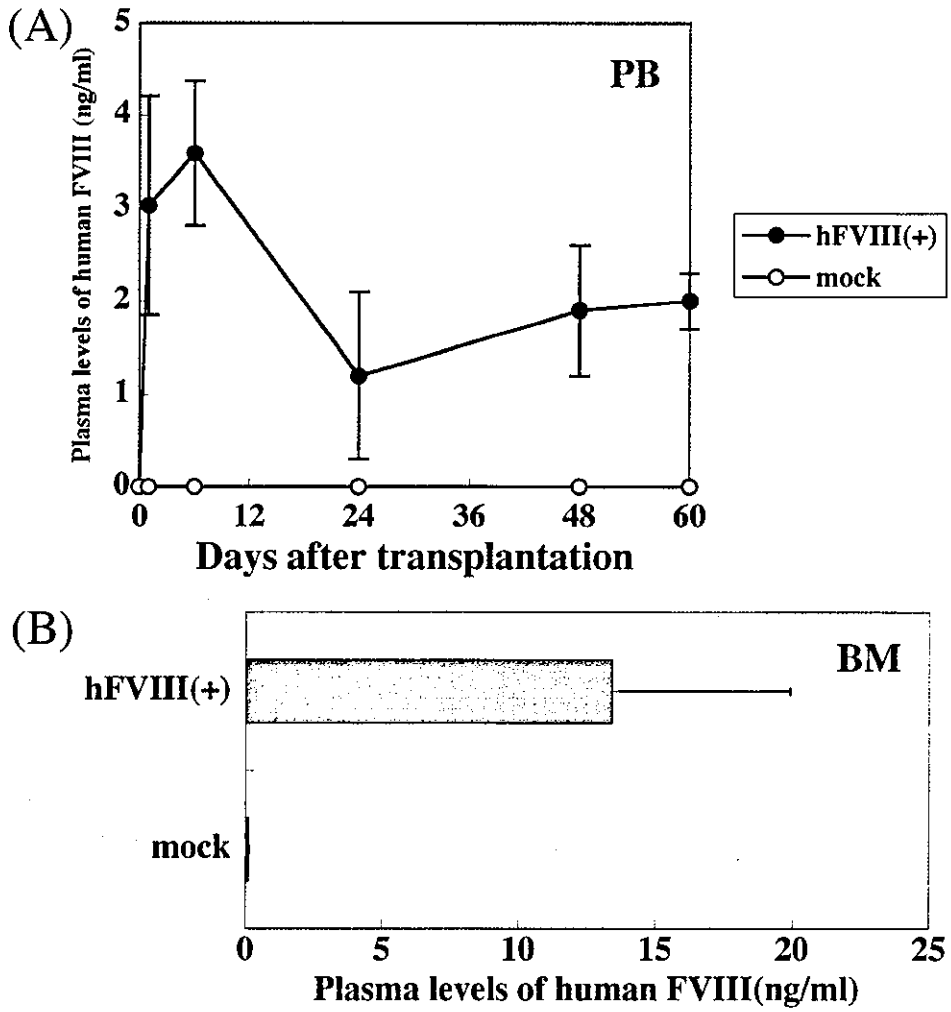

Figure 3. Plasma hFVIII levels in transplanted NOD/SCID mice. Peripheral blood was obtained from recipient mice on days 1, 6, 24, 48, and 60 after transplantation of CB-CD34$^+$ cells. Human FVIII concentrations in plasma (PB) of the NOD/SCID mice which received SIVhFVIII (closed circles) or mock (open circles) transduced CB-CD34$^+$ cells (A) and the hFVIII concentrations of the bone marrow preparation (BM) obtained on day 60 (B) are shown (mean ± SD, n = 3)

cells account for 56.9 ± 9.9% of mouse bone marrow cells. The average percentage of human cells expressing human CD34, CD19, CD33, or CD14 markers in the human CD45$^+$ cell fraction was 22.6 ± 3.7, 54.9 ± 7.9, 6.0 ± 0.8, or 10.3 ± 1.0%, respectively. No human CD3$^+$ T cells were detected in the mouse bone marrow samples. CD41$^+$ human platelets were found in not only 0.32 ± 0.06% of the peripheral blood platelets, but also in 16.4 ± 5.8% of the bone marrow platelets. Transduction of human CD34$^+$ cells by SIV vectors did not affect expression of lineage-specific markers in reconstituted peripheral blood cells, bone marrow cells, or spleen cells.

Detection of FVIII transcripts in bone marrow cells of NOD/SCID mice

To assess the expression of genes in engrafted bone marrow cells of NOD/SCID mice, bone marrow cells were harvested at 60 days after injection and subjected to RT-PCR analysis for detection of human BDD-FVIII transcripts. Total RNA extracted from bone marrow cells was subjected to PCR amplification using human FVIII, human GAPDH, or mouse GAPDH specific primers. As shown in Figure 5A, hFVIII transcripts were detected in bone marrow cells from the mice injected with hFVIII gene-transduced CB-CD34$^+$ cells (lanes 4, 5), but not detected from mock CB-CD34$^+$ cells (lanes 6, 7). Similarly, the hFVIII transcripts were observed in spleen cells and peripheral blood cells from mice engrafted for FVIII production, whereas the mock-transduced mice were negative. The transcripts of human GAPDH were detected in all cells (Figure 5B) derived from recipient mice, but not those from NOD/SCID mice without CD34$^+$ cell transplantation (Figure 5B, lane 3). Also the transcripts of mouse GAPDH were detected in all cells derived from NOD/SCID mice (Figure 5C, lanes 3–11). Human GAPDH transcripts were not detected in the liver, the lung, or the kidney (data not shown).

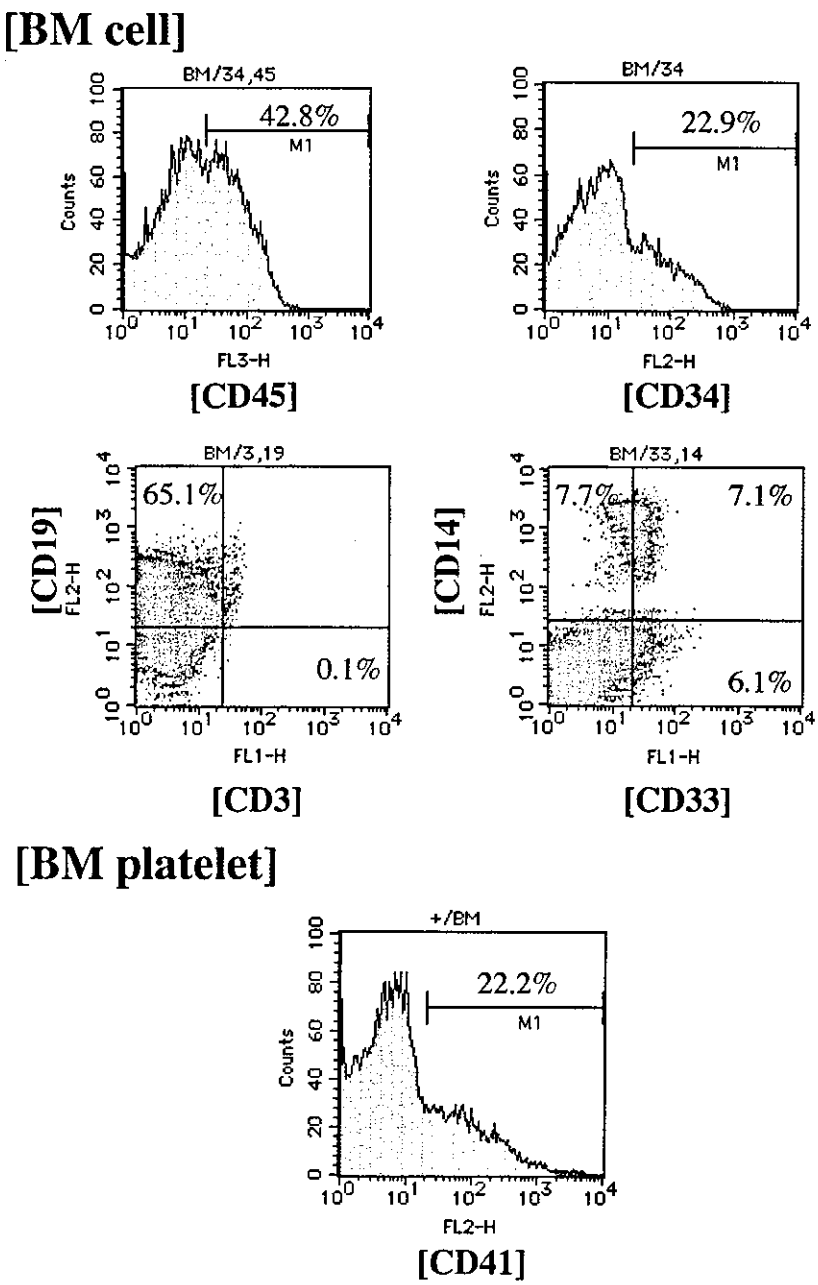

Figure 4. Expression of lineage markers in human CD45$^+$ cells and detection of human CD41$^+$ platelets in bone marrow cells. Expression of CD3, CD19, CD33, CD14, and CD34 in the human CD45$^+$ cells isolated from the bone marrow of a recipient mouse were analyzed by flow cytometry. Human platelets were detected by staining with RPE-conjugated anti-human CD41. The figure shows typical histograms of CD antigen expression on bone marrow cells obtained from NOD/SCID mouse on day 60 after transplantation with hFVIII-transduced CB-CD34$^+$ cells

Detection of hFVIII expressed in bone marrow cells and platelets of NOD/SCID mice

To detect hFVIII molecules in engrafted human-derived cells, mouse bone marrow cells were processed for detection of FVIII antigen in tissues using immunofluorescence. As shown in Figure 6, hFVIII was detected in bone marrow cells isolated from mice injected with SIVhFVIII-transduced CB-CD34$^+$ cells (Figure 6B), but not in cells from mice who received the mock-transduced CB-CD34$^+$ cells (Figure 6A). These data confirm the notion that the hFVIII was produced from the SIVhFIII-transduced cells. Upon sacrifice, platelets were collected from 1 mL of peripheral blood of recipient mice and extracted with 0.1 mL PBS containing Triton X-100 (0.5%). The platelet extracts were subjected to ELISA for quantification of hFVIII. We could detect 2 ng of hFVIII in platelets derived from 1 mL of recipient mouse peripheral blood.

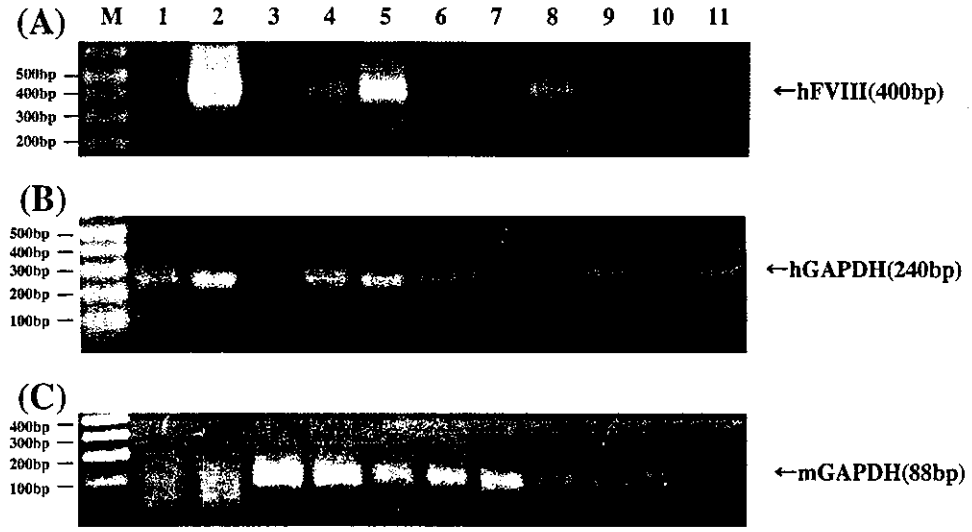

Figure 5. RT-PCR analysis of bone marrow cells. On day 60 after transplantation, RNA obtained from 5000 bone marrow cells was subjected to RT-PCR analyses with specific primer pairs for the human BDD-FVIII transcript (A), the human GAPDH transcript (B), and the mouse GAPDH transcript (C). PCR-amplified products were analyzed on 2% agarose gels followed by ethidium bromide staining (1, non-transduced CD34$^+$ cells; 2, SIVhFVIII-transduced CD34$^+$ cells; 3, NOD/SCID bone marrow; 4 and 5, recipient FVIII-transduced bone marrow cells; 6 and 7, mock-transduced bone marrow cells; 8, recipient spleen cells; 9, mock spleen cells; 10, recipient peripheral white blood cells; 11, mock peripheral white blood cells)

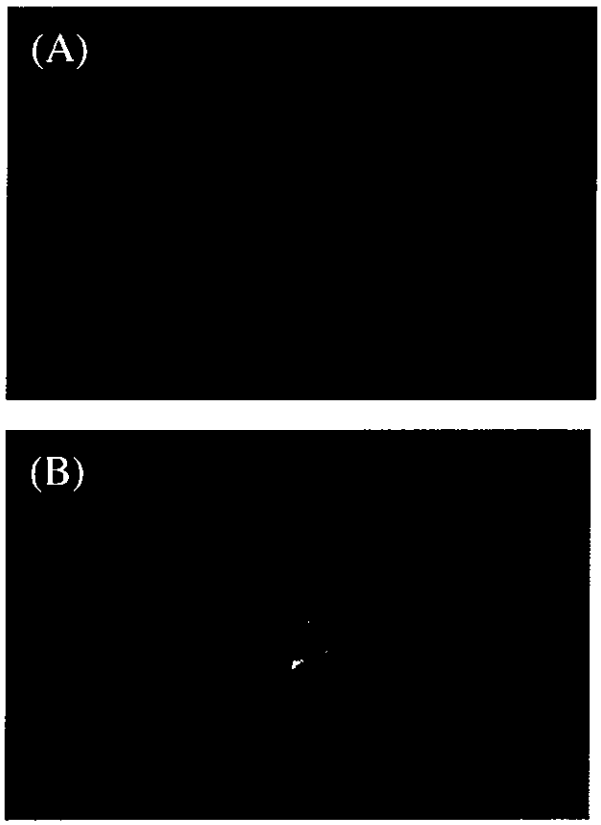

Figure 6. Immunofluorescent microscopy of hFVIII in bone marrow cells of the NOD/SCID mice. Bone marrow cells obtained from mock mice (A) or from recipient mice (B) were attached to glass slides using a Cytospin3. After fixation with 4% paraformaldehyde and washing with PBS, cells were incubated with sheep anti-hFVIII polyclonal antibodies. Bound antibodies were detected by AlexaFluor488-conjugated secondary antibody and visualized using a fluorescence microscope (E800; Nikon Co. Ltd., Tokyo, Japan)

Discussion

We have shown that SIV vectors carrying either eGFP or a therapeutic gene can transduce isolated CB-CD34$^+$ cells efficiently and that these cells can be transplanted into NOD/SCID mice successfully. We achieved high-level expression of human FVIII (hFVIII) in CB-CD34$^+$ cells transduced with SIVhFVIII *in vitro*, although VSVG-pseudotyped SIV vectors affected cell viability at high MOIs. Successful engraftment of SIV vector-transduced and FVIII-producing human CB-CD34$^+$ cells into NOD/SCID mice and the relatively low but effective expression level of the hFVIII antigen *in vivo* for 60 days were also achieved.

Hematopoietic stem cells are of considerable interest for gene therapy because of their self-renewal ability. Many reports have shown that hematopoietic stem cells are present in the CD34$^+$ cell fraction in humans and engraftment of human hematopoietic stem cells to mice is achievable by transplantation of CD34$^+$ cells into NOD/SCID mice. Previous reports showed that viral vector-transduced CB-CD34$^+$ cells could be engrafted in NOD/SCID mice [4–6]. However, *ex vivo* transduction of the FVIII gene to hematopoietic stem/progenitor cells by retroviral vector followed by transplantation into lethally irradiated normal or hemophiliac mice did not result in FVIII expression in the plasma, despite efficient engraftment of transduced cells [11–13]. Similarly, subcutaneous implantation of murine or human fibroblasts or bone marrow stromal cells transduced with hFVIII using retroviral vectors into immunodeficient mice resulted in long-term persistence of the engineered host cells *in vivo*, but no or only transient FVIII expression in plasma [24–26]. These disappointing results may well be

a result of inefficient transduction of the hematopoietic stem cells by the retroviral vectors.

Lentiviral vectors have been developed to overcome this inefficiency [7], with resultant transduction and integration of therapeutic genes into the target genome [4–6]. The commonly used lentiviral vectors are derived from HIV-1 or HIV-2 and endeavors have been made to make lentiviral vectors much safer [27]. However, the pathogenicity of HIV-based lentiviral vectors to humans is not clear especially in HIV carriers. Therefore, use of these vectors raises safety issues. The safety of HIV-derived vectors ultimately must be proven, but remains difficult because of the limited availability of animal models of HIV-induced diseases. The SIV lentiviral vectors used in this study were derived from SIVagmTYO1, non-pathogenic to its natural hosts or to experimentally infected Asian macaques [8], and no replication-competent virus particles were detected in vector-infected cells *in vitro*. Furthermore, the risk of development of replication-competent lentivirus particles in HIV carrier patients may be significantly lower than that for the HIV-1-based vectors because of the low sequence homology between HIV-1 and SIVagmTYO1. In this regard, SIVagmTYO1-based vectors have an advantage regarding safety issues and clinical application of gene therapy. To our knowledge, this is the first report of stable production of human FVIII in mice by hematopoietic cells reconstituted from CB-CD34$^+$ cells transduced with SIV vectors.

In the current study, the transduction efficiency of the CB-CD34$^+$ cells with the SIV vectors (Figure 1) was comparable to HIV-based lentiviral vectors [4]. Production of hFVIII (274.3 ± 20.1 ng/10^6 cells/24 h) by transduced CB-CD34$^+$ cells *in vitro* was considerable, raising the possibility of achieving therapeutic levels of plasma FVIII in the mice. After engraftment of transduced cells in NOD/SCID mice, plasma FVIII levels were maximal at 3.6 ± 0.8 ng/mL on day 6 after transplantation, declining gradually to a sustained level of 1.2 ng/mL for at least 60 days. The hFVIII production was observed in plasma and at the gene level in bone marrow cells. The hFVIII levels in plasma were lower than expected based on the *in vitro* production rate. One contributing factor may be the shorter half-life of hFVIII in mice compared with humans. The half-life of injected hFVIII in mice is approximately 1 h, whereas the half-life in hemophilia patients is closer to 8–12 h [25]. Chao *et al.* showed low-level production of hFVIII in immunocompetent C57BL/6 mice expressing a hFVIII inhibitor or in NOD/SCID mice without a detectable inhibitor. In these studies, FVIII levels increased after 10 months in both mice populations at the disappearance time of the inhibitor in the C57BL/6 mice [28]. Thus, secreted hFVIII was likely degraded in the NOD/SCID mice, analogous to that observed in the immunocompetent mice, resulting in low circulating levels of FVIII. It is also possible that the number of FVIII-producing cells decreased gradually after transplantation. We incubated CB-CD34$^+$ cells with SIVhFVIII at MOI of 50 vg/cell and approximately 50% of the CB-CD34$^+$ cells were transduced. These cells consist of hematopoietic stem cells and hematopoietic progenitor cells. During the early period after transplantation, the transduced cells produced hFVIII, as reflected by the relatively high level of plasma hFVIII in mice on days 1 and 6 after transplantation. After day 6, transduced human hematopoietic progenitor cells may have differentiated to progeny cells, which would be liberated from the bone marrow and cleared. Thus, the number of hFVIII-producing cells might be decreased after day 6 as they are derived solely from transduced human hematopoietic stem cells, their progeny and differentiated cells. The expected result would be declining plasma FVIII levels in the later periods of post-transplantation. It is also possible that silencing of the CMV promoter *in vivo* could have occurred, that in turn reduced FVIII production. The FVIII levels achieved in mice in this study were relatively low but such an increase of the FVIII level would develop clinical effects in hemophilias such as decrease of bleeding episodes and of use of FVIII concentrates. Data on clinical trials of hemophilia A gene therapy support this notion [29,30]. Therefore, we think that the FVIII levels achieved in this study were relatively low but an increase of FVIII to these levels would develop clinical improvement in severe hemophilia patients.

The replication mechanism of HIV-1 has been extensively studied in host cells. HIV-1 has the unique property among retroviruses to replicate in non-dividing cells. This property enables HIV-1 and other lentiviral-based vectors to transduce non-dividing hematopoietic stem cells. The central DNA flap of HIV-1 is thought to function as a cis-determinant of HIV-1 DNA nuclear import and to play a crucial role for lentiviral vector nuclear import and gene transduction of hematopoietic stem cells [31,32]. The SIVagm vectors used in this study were developed essentially according to the HIV-1-based vectors. Although SIVagm vectors are self-inactivating type vectors, the central DNA flap has not been included in the vectors as yet. We were able to transduce CD34$^+$ cells using SIVagm vectors efficiently *in vitro*, as shown in Figure 1, but FVIII production was decreased after transplantation. Thus, transgene integration into the CD34$^+$ cell genome by the SIVagmTYO1 vector might not occur efficiently. Currently, we are redesigning the SIVagmTYO1 vector to include the DNA flap. Use of such third-generation SIVagmTYO1 vectors will be of interest in future studies.

Analyses of lineage marker expression on the hematopoietic cells from the bone marrow and spleen of NOD/SCID mice confirmed engraftment and hematopoiesis of the transduced cells in the mice. Furthermore, we demonstrated CD41$^+$ platelets in the peripheral blood and the bone marrow, indicating that the human megakaryocytic progenitors could differentiate and mature to produce platelets in the mice. In fact, 2 ng of human FVIII were detected by ELISA in the platelet extracts derived from 1 mL of recipient mouse peripheral blood. These data also suggest that this is another advantage of transplantation of FVIII-producing hematopoietic stem cells, since the FVIII can be stored in platelets. These